



2017-08-01

MRI T2 Signal Changes Indicate Tau Pathophysiology in a Murine Alzheimer's Disease Model

Rajan Deep Adhikari
Brigham Young University

Follow this and additional works at: <https://scholarsarchive.byu.edu/etd>

 Part of the [Physiology Commons](#)

BYU ScholarsArchive Citation

Adhikari, Rajan Deep, "MRI T2 Signal Changes Indicate Tau Pathophysiology in a Murine Alzheimer's Disease Model" (2017). *All Theses and Dissertations*. 6944.
<https://scholarsarchive.byu.edu/etd/6944>

This Dissertation is brought to you for free and open access by BYU ScholarsArchive. It has been accepted for inclusion in All Theses and Dissertations by an authorized administrator of BYU ScholarsArchive. For more information, please contact scholarsarchive@byu.edu, ellen_amatangelo@byu.edu.

MRI T2 Signal Changes Indicate Tau Pathophysiology
in a Murine Alzheimer's Disease Model

Rajan Deep Adhikari

A dissertation submitted to the faculty of
Brigham Young University
in partial fulfillment of the requirements for the degree of
Doctor of Philosophy
Neuroscience

Jonathan J. Wisco, Chair
Richard K. Watt
Neal K. Bangerter
Scott R. Burt
Erin D. Bigler
Michael D. Brown

Department of Physiology and Developmental Biology
Brigham Young University

Copyright © 2017 Rajan Deep Adhikari

All Rights Reserved

ABSTRACT

MRI T2 Signal Changes Indicate Tau Pathophysiology in a Murine Alzheimer's Disease Model

Rajan Deep Adhikari

Department of Physiology and Developmental Biology, BYU

Doctor of Philosophy

Pathogenesis, diagnosis and treatment, the essential domains in medical practice, seem helpless to address Alzheimer's disease (AD). With a huge mortality rate, it is looming and threatening the socioeconomic barrier. Despite many different studies, the pathogenesis of AD remains inconclusive. However, growing numbers of studies suggest oxidative stress to contribute to the initiation and progression of AD. We propose an iron hypothesis: iron mediated oxidative damage by reactive oxygen species (ROS), which induces protective roles of amyloid beta and hyper-phosphorylated tau (HP-tau) to sequester iron and limit the disease. We propose to study such mechanism using transgenic mice models for AD, inducing oxidative stress to elevate intracellular iron, and analyze its co-localization with proteins using Magnetic Resonance Imaging (MRI), ¹H Nuclear Magnetic Resonance (NMR) spectroscopy and Western blot. We report three primary findings: 1) a significant loss in T2 signal over bilateral hippocampi of transgenic mice compared to the wild types (WT) by three months, corresponding to early disease and the ability of proteins to sequestration iron. Ability of rescue treatments to impede disease progression reflected as preserved T2 signal intensities over these areas throughout our study period of nine months. 2) Concentration of zinc and its dual role in the presence or absence of oxidative stress reflected as loss of ¹H NMR T2 measurement showed that higher concentrations of zinc were neuro protective when there was an active oxidative stress inducing condition, but neurotoxic and promote oxidative damage in normal condition. And 3) Different strains of mice, according to their transgene, expressed various proteins associated with AD. However, these expressions were in accordance with our iron-hypothesis.

Keywords: MRI, T2, Tau, Alzheimer's disease, oxidative stress, iron, amyloid beta, hyper phosphorylated tau, transgene, MRI, NMR, western blot, isoform.

ACKNOWLEDGMENTS

I would like to express my sincere appreciation to my advisor Dr. Jonathan J. Wisco for introducing the wonders and frustrations of scientific research. His persistent support, guidance, motivation and patience provided me with the holistic research experience important for my long-term career goals. He inspires me not only to grow as a research scientist, but also an avid thinker and a great teacher. I had the privilege of having independence in my work, which helped me to develop my individuality and self-sufficiency. He has been a great friend who understands my interests, necessities and limitations. He is one of the smartest, funniest and most compassionate advisors I know of. I hope I could live as enthusiastic and energetic a life as him, and someday be able to advise and influence others as I have been.

Beside my advisor, I would like to thank all other committee members Drs. Richard Watt, Scott Burt, Neal Bangerter, Michael Brown and Erin Bigler for their constant encouragement, comments, and willingness to help. My work would not have been possible without the combined effort from my committee. I appreciate and thank Dr. Dennis L. Eggett, for his time and help with statistics. I would like to thank my department chair Dr. Woodbury and all other faculty and staff for their assistance, which made this work possible.

My sincere thanks to BYU MRI-RF, Burt's NMR lab, Thomson's lab, Hansen's lab, Price's lab and Watt's lab for their space, supplies and technical support. I am extremely grateful for BYU animal husbandry team and IACUC for their help, comments and scrutiny. My special thanks to all undergraduate students helping me take on this mammoth task and my fellow colleagues for much needed humor and delight. Many credit to my friends and families for their warm wishes.

Heartfelt thanks to Reena, my wife, for her love, support, patience and understanding throughout this work. Delightful thanks to my wonderful son Reevan, who has always fueled in so much of joy and energy: that keeps me going.

Lastly, and most importantly, I would like to thank my parents Mr. Bamadev D. Adhikari and Mrs. Bishnu Adhikari. You receive my deepest gratitude and love for raising and nurturing me in a stable household with an unconditional love and dedication. It is impossible to thank you adequately for every selfless sacrifice you made. Your words of encouragement and push for tenacity are the very foundations for all my accomplishments. My successes have never been complete without your blessings. I dedicate this work to you.

TABLE OF CONTENTS

TITLE PAGE	i
ABSTRACT.....	ii
ACKNOWLEDGMENTS	iii
TABLE OF CONTENTS.....	v
LIST OF FIGURES	viii
LIST OF APPENDICES.....	ix
CHAPTER 1: Introduction	1
Iron Hypothesis:.....	10
Specific Aim 1	12
Specific Aim 2	13
Approach.....	13
Diet Treatments.....	13
Magnetic Resonance Imaging Protocol for Mice	13
Post-mortem Preparation and Analysis of Murine Brains	14
Western Blot Processing of Murine Brains	14
Nuclear Magnetic Resonance for Mice Brain.....	14
Material and Methods	15
Ethics Statement.....	15
Genotyping and Identification	15

Diet Treatments.....	15
References.....	17
CHAPTER 2: Hippocampal T2 Signal Loss During Aging in Transgenic Murine Modeled for AD Reflects Pathological Lesions.	24
Abstract.....	25
Introduction.....	25
Materials and Methods.....	27
Animals.....	27
Diet.....	27
Anesthesia.....	28
MRI Scanning.....	28
Estimation of Signal Intensities	29
Results.....	30
Discussion.....	32
Acknowledgements.....	33
References.....	35
CHAPTER 3: Dual Role of Zinc: NMR Relaxometry Measurements on Pathological and Normal Murine Brain.....	37
Abstract.....	38
Introduction.....	38
Materials and Methods.....	39

Inverse Recovery (T1)/Longitudinal Relaxation	40
CPMG (T2)/Spin-Spin Relaxation.....	41
Results.....	41
Discussion.....	45
Acknowledgements.....	46
References.....	48
CHAPTER 4: Strain Specific Regulation of Proteins: An Iron Hypothesis for Alzheimer’s Disease.....	50
Abstract.....	51
Introduction.....	51
Materials and Methods.....	53
Results.....	54
Ferritin.....	54
Tau isoforms	55
Tau Isoforms, Ferroportin and APP.....	55
Discussion.....	60
Acknowledgements.....	61
References.....	62
CHAPTER 5: General Conclusion and Relevance of Research.....	64
CURRICULUM VITAE.....	80

LIST OF FIGURES

Figure 1.1: Iron Regulation In Healthy Conditions.	5
Figure 1.2: Regulation Of Iron During Oxidative Stress.	9
Figure 2.1: T2 Weighted MRI Scan.	29
Figure 2.2: T2 Signal Intensities Over Left Hippocampus.	30
Figure 2.3: T2 Signal Intensities Over Right Hippocampus.	31
Figure 2.4: Estimated Marginal Means Of MRI.	31
Figure 3.1: Effect Of Rescue Treatments On Mean T1.	42
Figure 3.2: Effect Of Rescue Treatments On Mean T2.	43
Figure 3.3: Age Effect On Mean T1.	43
Figure 3.4: Age Effect On Mean T1 And T2:	44
Figure 3.5: Mean T1 And T2 Effect On Strain:	44
Figure 4.1: APP/PS1 And Tau Isoforms.	56
Figure 4.2: MAPT And Tau Isoforms.	56
Figure 4.3: WT And Tau Isoforms.	56
Figure 4.4: Strain Differences In Tau Isoforms.	57
Figure 4.5: APP/PS1 Response To Oxidative Stress.	57
Figure 4.6: MAPT Response To Oxidative Stress.	58
Figure 4.7: WT Response To Oxidative Stress.	58
Figure 4.8: Strain's Response To Oxidative Stress.	59
Figure 4.9: Ferritin Expression By Strain Type.	59

LIST OF APPENDICES

Appendix 1: T2 Signal Intensities Measurements From Bilateral Hippocampi And Eyes From All Strains Of Mice At One, Month.	65
Appendix 2: T2 Signal Intensities Measurements From Bilateral Hippocampi And Eyes From All Strains Of Mice At Three, Month.	67
Appendix 3: T2 Signal Intensities Measurements From Bilateral Hippocampi And Eyes From All Strains Of Mice At Six, Month.	69
Appendix 4: T2 Signal Intensities Measurements From Bilateral Hippocampi And Eyes From All Strains Of Mice At Nine, Month.	71
Appendix 5: T1 And T2 Measurements On Ultra-Centrifuged Mice Brain Homogenates For APP/PS1 Mice At Three, Six And Nine Months.	73
Appendix 6: T1 And T2 Measurements On Ultra-Centrifuged Mice Brain Homogenates For MAPT Mice At Three, Six And Nine Months.	74
Appendix 7: T1 And T2 Measurements On Ultra-Centrifuged Mice Brain Homogenates For WT Mice At Three, Six And Nine Months.	75
Appendix 8: Ultra-Centrifuged Mice Brain Homogenates Were Run On SDS PAGE Gel And Were Probed And Density Measured For Following Proteins: APP, Ferritin, Ferroportin And GAPDH.	76
Appendix 9: Ultra- Centrifuged Mice Brain Homogenates Were Run On SDS PAGE Gel And Were Probed For Various Following Proteins. Density Measurement Of GAPDH For Tau And Different Tau Proteins Measured At 42, 45 And 48 kDa.	78

CHAPTER 1: Introduction

Alzheimer's disease (AD) is a progressive and incurable neurodegenerative disorder that is the sixth leading cause of death in United States. It accounts for almost 60 to 80 percent of all forms of dementia. One in three senior citizens in United States die with AD or other forms of dementia. However, commonly seen in the elderly population over the age of 65, age being the biggest risk factor, Alzheimer's disease is not a normal aging issue (Association 2017). With new developments and innovations, there has been a significant decrease in other leading causes of death, while the mortality from AD has increased by 89% since 2000. This disease is estimated to cost the nation around 1.1 trillion by 2050 (Association 2017). There is no specific investigation method to confirm the diagnosis of AD except by post mortem brain biopsy showing amyloid plaques and neurofibrillary tangles (Dickson 1997, Braak and Braak 1998). Progression of neurodegeneration and worsening of AD are irreversible. However, some symptomatic treatments can impede disease progression to improve the quality of life for those with the disease and their caregivers (Association 2017).

Depositions of extracellular senile plaques, primarily mediated by amyloid beta ($A\beta$), and development of intracellular neurofibrillary tangles are the hallmarks of this disease. These plaques and tangles in turn promote degeneration of neuronal synapses, which is progressive, and irreversible (Butterfield and Boyd-Kimball 2004, Ittner, Ke et al. 2010). These events are primarily seen in the neocortex, hippocampus and other subcortical regions involved in cognitive function (Moreira, Carvalho et al. 2010). These pathological changes occur many years prior to any clinical symptoms making them ideal markers to predict AD (Nordberg 2008).

Amyloid B peptide is a normal physiological product from proteolytic processing of its precursor protein known as Amyloid Precursor Protein (APP). APP is a transmembrane protein

whose precise function is unknown but its overexpression shows a positive effect on cell health and growth (O'Brien and Wong 2011). An APP protein undergoes normal proteolytic processing by α and γ -secretase respectively (nonamyloidogenic pathway), producing products promoting normal cellular functions. Those APPs who fail to be processed normally are internalized inside the cell and are cleaved by beta site APP cleaving enzyme (BACE) and γ secretase (amyloidogenic pathway) generating A β (Younkin 1998, Greenfield, Tsai et al. 1999). Generally, such enzymatic actions produce variable length of A β with mostly 40 (A β 40) and 42 (A β 42) amino acid residues respectively. The most abundant residue is A β 40, with around 5-15% of A β 42 (Durkin, Murthy et al. 1999). Normally in young and healthy brains, these residues are tightly regulated (Shankar and Walsh 2009), however, in old and pathological brains, the A β oligomers are shown to aggregate and start disease progression promoting neuronal dysfunction (Harkany, Abraham et al. 2000, Qiu, Kivipelto et al. 2009, Bao, Wicklund et al. 2012). Presenilin genes 1 (PSEN1) and 2 (PSEN2) regulate enzymatic function of γ -secretase, and any defect or mutation in these genes leads to increase formation of A β as seen in early onset forms of AD (Ridge, Ebbert et al. 2013).

Tau is a microtubule-associated protein, which is important in the assembly and stabilization of microtubules (Weingarten, Lockwood et al. 1975). They also influence motor proteins like kinesin and dynein that regulate anterograde and retrograde axonal transport respectively (Stamer, Vogel et al. 2002). They constitute a family of six isoforms, which range from 352 to 441 amino acids. Isoforms differ due to presence of three or four repeat regions (3R,0;4R,0;3R,29;4R,29;3R,58;4R,58), found at the carboxyl terminal and presence or absence of two peptide inserts at amino terminal (Buee, Bussiere et al. 2000). Three isoforms of Tau containing exon 10 (4R) are more efficient at promoting microtubule assembly (Goedert and

Jakes 1990), while the isoforms that lack exon 10 (3R) are found to be associated with AD (Espinoza, de Silva et al. 2008). Unlike natively unfolded tau, aggregated tau proteins that form into paired helical filaments (PHFs) and into neurofibrillary tangles (NFTs) are associated with tauopathies: which is characteristic of various neurodegenerative diseases (Lee, Goedert et al. 2001). Tau is vital for A β induced neurotoxicity (Roberson, Scarce-Levie et al. 2007) and that the tau pathology can spread between neurons (Holmes and Diamond 2014). However, while it is predominantly an intracellular protein, many recent experiments suggest physiological release of tau proteins into the extracellular spaces. Moreover, neuronal activity regulates these processes (Pooler, Phillips et al. 2013, Yamada, Holth et al. 2014). Tau functions are regulated by its phosphorylation state, and the tau proteins, found in the PHFs that form NFTs, which formed these filaments were abnormally phosphorylated (Grundke-Iqbal, Iqbal et al. 1986, Grundke-Iqbal, Iqbal et al. 1986, Kosik, Joachim et al. 1986). This hyper-phosphorylation disrupts normal function of tau suggesting its role in pathogenesis of tauopathies by inducing microtubule network breakdown by neuritic atrophy and neurodegeneration. Studies of tau in patients with tauopathies or in transgenic mice show hyper phosphorylation of tau preceding aggregation (Braak, Braak et al. 1994). Other notable loss of functions, following hyper-phosphorylation of tau include but are not limited to iron transport, neurogenesis, long term depression (LTD) and DNA protection (Chauhan and Chauhan 2006, Sultan, Nessler et al. 2011, Lei, Ayton et al. 2012).

Many theories have been put forward to elucidate the pathogenesis of AD; however, they still cannot fill the huge gap in our understanding. Nevertheless, many studies have emphasized the importance of oxidative stress in the pathogenesis of neurodegenerative illness. In normal physiological conditions, oxygen radicals are regulated by antioxidants. However,

during pathological conditions, this balance is altered, producing uncontrollable reactive oxygen species (ROS) which are toxic to neurons. The oxidative damage seen in AD includes, but is not limited to, advanced glycation products (AGE) (Niwa, Katsuzaki et al. 1996, Zhou, Miller et al. 1998), nitration (Good, Werner et al. 1996) and lipid peroxidation (Sultana, Perluigi et al. 2013). There has been an interesting debate whether A β and NFTs are a major source of oxidative free radicals promoting neurodegeneration, or that they both serve to compensate or reduce oxidative damage (Hensley, Carney et al. 1994). This hypothesis of A β as an antioxidant is seen in patients with Down's syndrome, where A β deposits are developed in late teens in response to increased oxidative stress (Cenini, Dowling et al. 2012). There seems to be equal strength in the debate regarding A β and NFTs as precursors of oxidative damage or formed as a response to such insults. Many observations provide proof that metals, such as iron (Hare, Ayton et al. 2013), aluminum (Crapper, Quittkat et al. 1980), mercury (Xu, Farkas et al. 2012), copper (Brewer 2014) and zinc (Deibel, Ehmann et al. 1996) play a major catalytic role in production of free radicals, and much attention has revolved around iron.

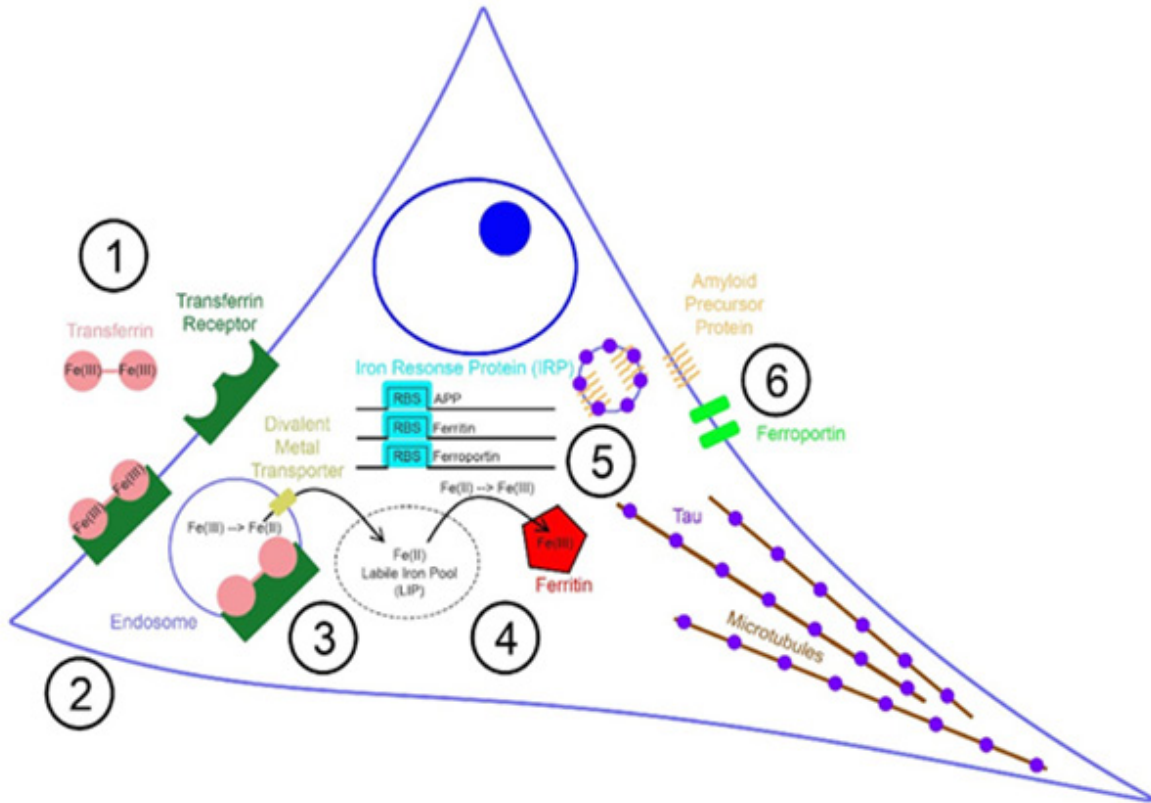


Figure 1.1: Iron Regulation In Healthy Conditions. For healthy neurons, 1) Fe^{3+} is transported by iron transport protein “transferrin”, which recognizes the “transferrin receptor” on the cell surface and binds to it. 2) This protein-receptor complex goes through endocytosis into an endosome. 3) Low pH inside endosome reduces Fe^{3+} to Fe^{2+} . Fe^{2+} is then exported to the cytosol via divalent metal transporter (DMT). Fe^{2+} enters the labile iron pool (LIP). 4) This form of iron is used for normal enzymatic functions; otherwise, it is oxidized back to Fe^{3+} and is sequestered by iron storage protein “ferritin”. 5) The LIP is monitored by iron response proteins (IRPs) that control expression of several iron proteins (APP, Ferritin, and Ferroportin), by binding to a hairpin loop in the mRNA known as iron response elements (IRE) and block the ribosome-binding site to prevent over translation of these proteins. 6) Indeed, there is a normal expression of APP, Ferritin and Ferroportin. APP and Ferroportin work together to reduce the levels of intracellular and extracellular iron.

Iron is an essential micronutrient whose metabolism is tightly regulated. Exchange and transport of iron is mediated by Transferrin (Tf), an 80-kDa protein (Anderson, Baker et al. 1987). Ferrous ions (Fe^{2+}) are oxidized by ferroxidase to Ferric ions (Fe^{3+}) before being exported out of cell into the interstitium via ferroportin (FPN), a transmembrane protein (Aisen, Enns et al. 2001). These Ferric ions (Fe^{3+}) are incorporated into Tf and are circulated (Finch and Huebers 1982). The blood brain barrier prevents such complexes from diffusing into the nervous membrane; however, there seems to be another mechanism of endocytosis in the brain capillary endothelial cells (Moos, Rosengren Nielsen et al. 2007, Hare, Ayton et al. 2013). The Tf Fe^{3+} complexes are recognized by Tf receptors and are internalized into the endosomes. Low pH inside endosome, converts Ferric to Ferrous ions, which are then expelled out into the cytosol through Divalent Metal Transporter 1 (DMT1) (Hentze, Muckenthaler et al. 2004). These free iron molecules in the cytosol constitute what is known as labile iron pool (LIP), used for normal physiological functions. Iron can be stored in a storage protein called ferritin (F) (Theil 2004). Any excess iron is exported out to interstitium by the only known iron exporting protein, FPN (Ganz 2005), which is associated with ferroxidase and helps to oxidize ferrous to ferric ions (Abboud and Haile 2000). Neurons are devoid of ferroxidase, but APP substitutes their function in regulating iron levels (Duce, Tsatsanis et al. 2010). Iron is shuttled between ferritin and LIP to maintain a constant level for cellular functions. These functions are regulated by Iron response proteins (IRP 1 & IRP 2), which are peptides that bind with iron response elements (IRE) at the ribosomal binding sites (RBS) (Aisen, Enns et al. 2001) of amyloid precursor protein (APP), ferritin and ferroportin, preventing their expression. IRP are closely regulated by LIP (54) (Figure 1.1). Disruptions in these regulations are found to promote neurodegeneration illnesses, like AD (Qin, Zhu et al. 2011, Antharam, Collingwood et al. 2012), where they are found to be

associated with amyloid plaques and neurofibrillary tangles (Connor, Menzies et al. 1992, Smith, Harris et al. 1997). Neurons were found to have high levels of iron, in their redox active state (Good, Werner et al. 1996, Smith, Harris et al. 1997) prior to formation of plaques (Leskovjan, Kretlow et al. 2011) , which were prevented by iron chelation therapy (Guo, Wang et al. 2013).

The brain requires around 20% of basal oxygen consumption. During respiration, mitochondria, which are regulated by superoxide dismutase, produce superoxide as a byproduct. As discussed earlier, iron is recognized as a major cause of oxidative stress due to its potential in forming hydroxyl radicals from hydrogen peroxide (Fenton reaction) (Honda, Casadesus et al. 2004). Immunohistochemistry studies have shown co-localization of iron with amyloid plaques (A β) and hyper-phosphorylated Tau proteins (Stamer, Vogel et al. 2002, Mondragon-Rodriguez, Perry et al. 2013). Such co-localizations of iron with amyloid beta were reported using an ingenious method using Magnetic Resonance Imaging (MRI) (Meadowcroft, Connor et al. 2009).

In our work here, we hypothesize that A β and HP-tau sequester excess iron that overwhelms ferritin: primary iron storage protein (Watt 2013). Since, iron can be associated with various proteins; we want to know the affinity of iron to the different proteins involved during different stages of disease. Our proposed iron hypothesis for AD may clarify this affinity. We hypothesize that A β and P-tau actually protect neurons against oxidative damage by binding to iron. However, we do not fully understand the pathophysiological mechanism or related stages of disease with regard to A β and P-tau iron sequestration.

Homocysteine is known to be a neurotoxic non-protein amino acid (Kruman, Culmsee et al. 2000), and is known to be elevated in AD (Miller 1999). Its neurotoxicity is mediated via

mechanisms like stimulating NMDA (Lipton, Kim et al. 1997) and glutamate receptors (Kruman, Culmsee et al. 2000). Homocysteine is also known inhibit and mobilize iron from ferritin promoting iron mediated oxidative damage. We propose that neurons sense this elevated free iron and promote production of ferritin, amyloid beta and neurofibrillary tangles to sequester them and prevent further oxidative damage. We believe that it is a natural defense mechanism of neurons against oxidative insult. We surmise that formation of amyloid beta outside the neurons is natural mechanism to keep free iron outside the cells, and when this mechanism overwhelms; the tau protein gets hyper-phosphorylated to attract more free iron, thereby trying to save neurons from further damage.

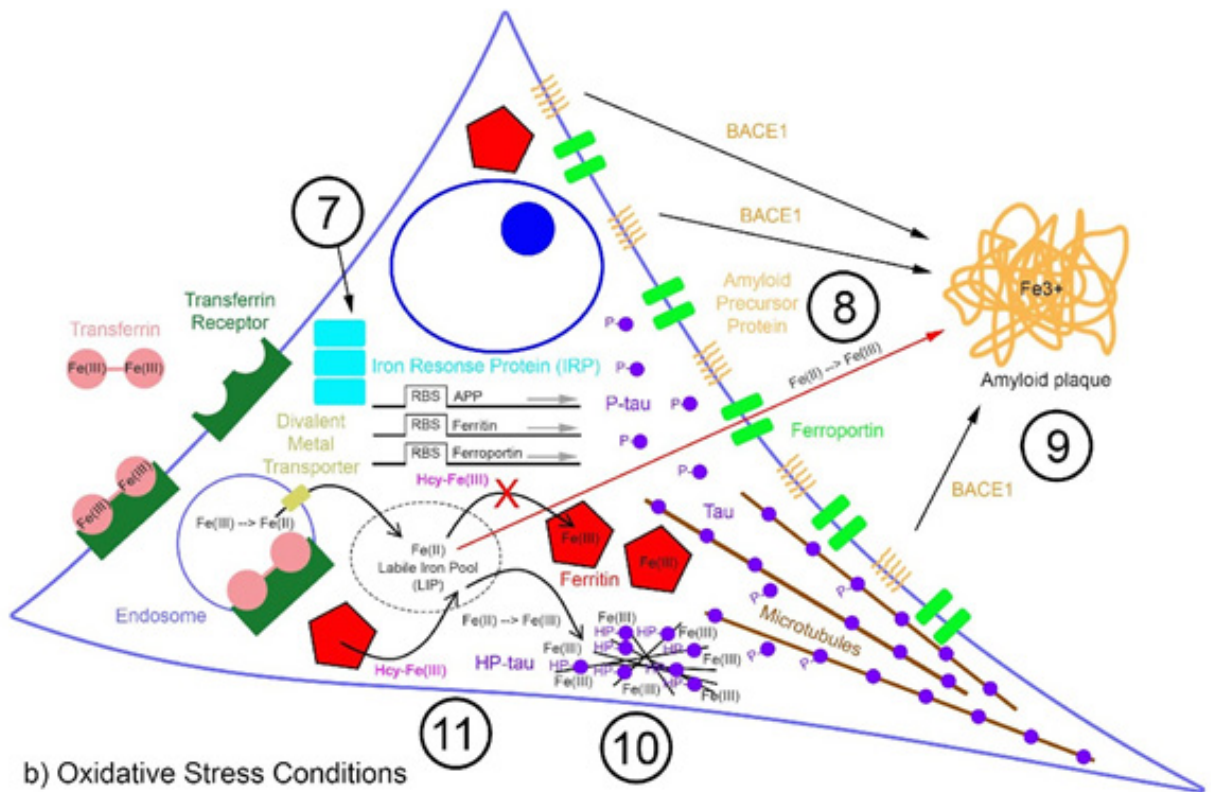


Figure 1.2: Regulation Of Iron During Oxidative Stress.

Elevated iron levels cause significant changes in the controlled environment inside the cell. 7) When iron levels rise, the IRPs recognize the elevated iron levels and fall off the IRE to allow transcription of APP, Ferritin and Ferroportin. If the increase in iron level is transient, increased Ferritin expression is able to bind and sequester the iron and prevent oxidative stress caused by free iron. 8) If the neuron is experiencing oxidative stress and free iron load, it promotes phosphorylation of tau (p-tau). Tau normally controls the trafficking of APP to cell surface. Phosphorylated tau allows APP to fuse with the membrane where it couples with Ferroportin to export iron, preventing reactive oxygen species formation. 9) Continued oxidative stress induces the expression of BACE1, the protease that cleaves APP to form Ab, which then binds and packs free iron into plaques. Continued neuronal oxidative stress leads to inhibition of phosphatase, which cycles p-tau to tau. This leads to hyper-phosphorylation of tau (HP-tau), which is known to form aggregates with trivalent metals such as Fe³⁺. 10) According to this model, elevated Fe³⁺ levels exist and trigger the aggregation of HP-tau into tangles. 11) We propose that the homocysteine (Hcy) is the trigger that leads to the initial oxidative stress. Hcy blocks iron loading into Ferritin, releases iron from Ferritin and hyper-phosphorylates tau.

Iron Hypothesis:

Our iron hypothesis as a cause for AD is based on the facts that iron reacts with oxygen to generate what is known as reactive oxygen species (ROS) which promotes oxidative damage to tissues, and that iron is associated with A β plaques, HP-tau tangles in, and AD diseased brain. Figure 1.2 demonstrates regulation of iron during oxidative stress. Homocysteine (Hcy) is a molecule known to be elevated in several conditions including AD. Hcy can perform redox chemistry to reduce and release iron from ferritin leading to elevated cytosolic iron levels. Hcy also inhibits iron loading into ferritin by binding to iron. The overall effect is an elevated level of free iron in the cytosol. The excess of iron is then expelled from the cell via Ferroportin, which requires APP for better coordination. Thus, the elevated iron level will release the IRB from RBS promoting expression of APP, ferritin and Ferroportin. The APP is cleaved by secretase to form A β that sequesters iron outside the cells. Hcy inhibits phosphatase activity and that continuous oxidative stress causes phosphorylation of tau (HP-tau), which is released from microtubules leading to its aggregations. When the export of iron to A β plaques becomes overwhelmed, the HP-tau comes into play by storing the excess iron in the tangles, within the cells. Tau is the microtubule-associated protein that undergoes dynamic phosphorylation and de-phosphorylation as it maintains the integrity of the microtubules. Under various oxidative conditions, this dynamic cycle is altered and tau proteins undergo hyper-phosphorylation. In AD, HP-tau leads to the formation of paired helical filaments and neurofibrillary tangles inside the cells.

One function of tau is to traffic APP to the cell surface. Phosphorylation of tau allows APP to fuse with the membrane where it couples with Ferroportin to export iron from the neuron to protect from the formation of reactive oxygen species. Continued oxidative stress induces the

expression of BACE1, the protease that cleaves APP to form A β , then A β binds and packages free Fe³⁺ into plaques. Continued neuronal oxidative stress leads to inhibition of phosphatases, which cycle P-tau back to tau. This leads to hyper-phosphorylation of tau (HP-tau), which is known to form aggregates with Fe³⁺. According to our model, elevated Fe³⁺ levels exist and trigger the aggregation of HP-tau into tangles. We propose that homocysteine (Hcy) is the trigger that leads to the initial oxidative stress. Hcy blocks iron loading into ferritin, releases iron from ferritin, and causes the hyper-phosphorylation of tau.

We propose to conduct experiments to test the pathophysiological process of oxidative stress and development of AD pathology on a murine animal model. We will introduce oxidative stress conditions through the administration of a methionine rich diet, which provides a non-protein amino acid –Homocysteine. In separate, age- matched cohorts; we will introduce metformin, zinc and Clioquinol, each of which acts directly to reduce the free iron in the cell. Metformin is known to reduce rate of formation of advance glycation products (AGEs) (Ahmad, Shahab et al. 2013), decrease xanthine oxidase activity (Pavlovic, Kocic et al. 2000) and lipid peroxidation markers (Tessier, Maheux et al. 1999) improving antioxidant activities in red blood cells (Faure, Rossini et al. 1999) and hepatic and blood vessels (Ewis and Abdel-Rahman 1995).

Clioquinol is an antibiotic and naturally present copper/zinc chelator that solubilizes amyloid beta deposits (Faux, Ritchie et al. 2010). A phase II clinical trial with Clioquinol reported significant less deterioration in cognitive function with patients with moderately severe AD (Ritchie, Bush et al. 2003). It has higher affinity for iron (Todorich and Connor 2004) and reduces brain iron content (Kaur, Yantiri et al. 2003).

Zinc is an essential micronutrient required for intracellular signaling; cell mediated immune functions and oxidative stress (Gammoh and Rink 2017). Zinc inhibits nicotinamide

adenine dinucleotide phosphate oxidases (NADPH oxidase), which catalyzes the production of ROS (Marreiro, Cruz et al. 2017). It also serves as a cofactor of superoxide dismutase (SOD), which catalyzes ROS into hydrogen peroxidase. It also helps induce generation of metallothione, which can scavenge ROS (King, Brown et al. 2016). Zinc increases the activation of antioxidant proteins, molecules and enzymes such as glutathione (GSH), catalase, and SOD. It also reduces the activities of oxidant-promoting enzymes such as inducible nitric acid synthase and NADPH oxidase and inhibits the lipid peroxidation products.

We hypothesize that treatment with these drugs would indirectly reduce the pathological burden seen in AD. These experimental perturbations will be introduced regularly throughout the animals' lifetimes, and analyzed at one, three, six and nine months of age using in vivo imaging, postmortem immunohistochemistry, and biochemistry techniques.

We propose the following specific research questions to support our specific aims:

Specific Aim 1

We will elucidate the time course of iron association with APP, Ferroportin, ferritin, A β and HP-tau proteins in wild type and AD transgenic murine brains by introducing controlled oxidative stress conditions through the administration of homocysteine. We want to know specifically: Does the temporal, sequential pathophysiology related to oxidative stress influence neuronal death? In addition, we will introduce a subset of mice subjects to metformin, Clioquinol, and zinc treatments, which are known or proposed to reduce the labile iron pool (LIP) in models of oxidative stress. We expect our iron-reducing treatments to ameliorate the deposition of iron-bound A β and ironbound HP-tau even in transgenic AD mice (beyond what they would have genetically deposited).

Specific Aim 2

We will develop an MRI technique to differentiate iron-bound A β and iron-bound HP-tau in our murine brains. We want to know if we can differentiate iron-bound A β localization from iron bound HP-tau localization using MRI technique and develop an anatomical and pathological biomarker for AD.

Our experimental plan and procedures are designed to test our Iron Hypothesis, but our plan also tests treatments known to decrease cellular iron. If our hypothesis is correct, the work in this proposal will prove our hypothesis and outline a pathway for preventive treatments to lower intracellular iron concentrations to prevent AD.

Approach

Diet Treatments

Starting at 1 month of age, half of the mice from each strain type will receive either methionine rich chow while the other half will continue with regular food. Oxidative stress rescue treatments with Metformin, Zinc and Clioquinol will start at 3 months, amelioration of oxidative stress pathology is expected to begin appearing at 6 months relative to non-rescued mice.

Magnetic Resonance Imaging Protocol for Mice

We will acquire MRI images of the mice, at 1, 3, 6 and 9 months of age, in a Siemens 3T Trio scanner. Mice will be anesthetized using isoflurane and placed in a custom-made 4-turn Transmit/Receive (TR) solenoidal RF mouse coil. We expect T2 signal loss in hippocampi as plaques and iron in them will build up generating contrast image. Such signal loss will be related

with the western blot analysis. These optimizations and relations will help us to develop an MRI technique, which can differentiate ironbound A β and ironbound HP-tau.

Post-mortem Preparation and Analysis of Murine Brains

At the end of each time point, one subgroup of mice will be sacrificed. Brains will be extracted and hemispheres will be separated, with one processed for histological analysis and the other processed for Western blot and NMR analysis. We will correlate with MRI scans to locate the pathological lesion and will biopsy the brain specimen for NMR and western blot experiments.

Western Blot Processing of Murine Brains

The biopsies will be homogenized and ultra-centrifuged to be analyzed by Western blot procedures and analyzed by antibodies specific for APP, Ferroportin, A β , tau and ferritin. SDS gel electrophoresis will separate different proteins based on their molecular weight. Western blot then can help us identify relative quantities for a particular protein or proteins of interest. We expect to see the expression of proteins like APP, Ferroportin, A β , HP-tau and ferritin to increase after oxidative stress conditions and reduce following rescue treatments.

Nuclear Magnetic Resonance for Mice Brain

We will run NMR on the same biopsy samples and measure relaxation properties. We will use these values to inform MRI scans at subsequent time points for cohort subgroups and develop a technique to differentiate ironbound A β and ironbound HP-tau in our murine brains.

Material and Methods

Ethics Statement

Institutional Animal Care and Use Committee (IACUC) approved all procedures and all animals were treated in accordance with their guidelines. Three strain types 1: B6.Cg-Mapttm1 (GFP) Klt Tg(MAPT)^{8cPdav}/J 18 mice (7F, 11M) were bred by crossing mice that are homozygous for the targeted mutation- MAPT and hemizygous for the transgene- human MAPT with mice homozygous for targeted mutation- MAPT and wild type for the transgene. 2: C57BL/6J were purchased from Jackson lab and 3: B6.Cg-Tg (APP695) 3Dbo Tg(PSEN1^{dE9})S9Dbo/Mmjax were purchased from Mutant mouse resources and research centers. They were maintained in specific pathogen free environment at Life Science Building, BYU. They were fed on regular ad libitum (TD.8604) and were housed at a 12-hour light/12-hour dark cycle. They were bred and the pups were genotyped for their respective transgene at 21 days of age. Matched genotypes were separated for experiment and unmatched genotypes were culled as per IACUC guidelines.

Genotyping and Identification

Ear notching method was used to collect tissues for DNA sampling for genotyping and identification. Proper techniques were ensured to restrain the animal during ear notching. The notching device was disinfected using 75% ethanol between each animal and between cages.

Diet Treatments

At one month of age, 9 mice from each strain type were separated randomly to receive methionine rich ad libitum (36 mg/day), the other half were continued on control ad libitum (methionine: 18 mg/day).

After two months, all mice received rescue treatment with metformin, zinc or Clioquinol in continuation with the diets they were receiving.

1. 0.1% Metformin.
2. 30 mg/kg/day Clioquinol.
3. 200mg/kg zinc. (control diet: 80mg/kg)

References

- Abboud, S. and D. J. Haile (2000). "A novel mammalian iron-regulated protein involved in intracellular iron metabolism." *J Biol Chem* 275(26): 19906-19912.
- Ahmad, S., U. Shahab, M. H. Baig, M. S. Khan, M. S. Khan, A. K. Srivastava, M. Saeed and Moinuddin (2013). "Inhibitory effect of metformin and pyridoxamine in the formation of early, intermediate and advanced glycation end-products." *PLoS One* 8(9): e72128.
- Aisen, P., C. Enns and M. Wessling-Resnick (2001). "Chemistry and biology of eukaryotic iron metabolism." *Int J Biochem Cell Biol* 33(10): 940-959.
- Anderson, B. F., H. M. Baker, E. J. Dodson, G. E. Norris, S. V. Rumball, J. M. Waters and E. N. Baker (1987). "Structure of human lactoferrin at 3.2-A resolution." *Proc Natl Acad Sci U S A* 84(7): 1769-1773.
- Antharam, V., J. F. Collingwood, J. P. Bullivant, M. R. Davidson, S. Chandra, A. Mikhaylova, M. E. Finnegan, C. Batich, J. R. Forder and J. Dobson (2012). "High field magnetic resonance microscopy of the human hippocampus in Alzheimer's disease: quantitative imaging and correlation with iron." *Neuroimage* 59(2): 1249-1260.
- Association, A. s. (2017). "2017 Alzheimer's Disease Facts and Figures."
- Association, A. s. (2017). "What Is Alzheimer's." *Alzheimer's and dementia basics* Retrieved June 1, 2017, 2017, from http://www.alz.org/alzheimers_disease_what_is_alzheimers.asp.
- Bao, F., L. Wicklund, P. N. Lacor, W. L. Klein, A. Nordberg and A. Marutle (2012). "Different beta-amyloid oligomer assemblies in Alzheimer brains correlate with age of disease onset and impaired cholinergic activity." *Neurobiol Aging* 33(4): 825.e821-813.
- Braak, E., H. Braak and E. M. Mandelkow (1994). "A sequence of cytoskeleton changes related to the formation of neurofibrillary tangles and neuropil threads." *Acta Neuropathol* 87(6): 554-567.
- Braak, H. and E. Braak (1998). "Evolution of neuronal changes in the course of Alzheimer's disease." *J Neural Transm Suppl* 53: 127-140.
- Brewer, G. J. (2014). "Alzheimer's disease causation by copper toxicity and treatment with zinc." *Front Aging Neurosci* 6: 92.
- Buee, L., T. Bussiere, V. Buee-Scherrer, A. Delacourte and P. R. Hof (2000). "Tau protein isoforms, phosphorylation and role in neurodegenerative disorders." *Brain Res Brain Res Rev* 33(1): 95-130.
- Butterfield, D. A. and D. Boyd-Kimball (2004). "Amyloid beta-peptide(1-42) contributes to the oxidative stress and neurodegeneration found in Alzheimer disease brain." *Brain Pathol* 14(4): 426-432.

- Cenini, G., A. L. Dowling, T. L. Beckett, E. Barone, C. Mancuso, M. P. Murphy, H. Levine, 3rd, I. T. Lott, F. A. Schmitt, D. A. Butterfield and E. Head (2012). "Association between frontal cortex oxidative damage and beta-amyloid as a function of age in Down syndrome." *Biochim Biophys Acta* 1822(2): 130-138.
- Chauhan, V. and A. Chauhan (2006). "Oxidative stress in Alzheimer's disease." *Pathophysiology* 13(3): 195-208.
- Connor, J. R., S. L. Menzies, S. M. St Martin and E. J. Mufson (1992). "A histochemical study of iron, transferrin, and ferritin in Alzheimer's diseased brains." *J Neurosci Res* 31(1): 75-83.
- Crapper, D. R., S. Quittkat, S. S. Krishnan, A. J. Dalton and U. De Boni (1980). "Intranuclear aluminum content in Alzheimer's disease, dialysis encephalopathy, and experimental aluminum encephalopathy." *Acta Neuropathol* 50(1): 19-24.
- Deibel, M. A., W. D. Ehmann and W. R. Markesbery (1996). "Copper, iron, and zinc imbalances in severely degenerated brain regions in Alzheimer's disease: possible relation to oxidative stress." *J Neurol Sci* 143(1-2): 137-142.
- Dickson, D. W. (1997). "Neuropathological diagnosis of Alzheimer's disease: a perspective from longitudinal clinicopathological studies." *Neurobiol Aging* 18(4 Suppl): S21-26.
- Duce, J. A., A. Tsatsanis, M. A. Cater, S. A. James, E. Robb, K. Wikke, S. L. Leong, K. Perez, T. Johanssen, M. A. Greenough, H. H. Cho, D. Galatis, R. D. Moir, C. L. Masters, C. McLean, R. E. Tanzi, R. Cappai, K. J. Barnham, G. D. Ciccotosto, J. T. Rogers and A. I. Bush (2010). "Iron-export ferroxidase activity of beta-amyloid precursor protein is inhibited by zinc in Alzheimer's disease." *Cell* 142(6): 857-867.
- Durkin, J. T., S. Murthy, E. J. Husten, S. P. Trusko, M. J. Savage, D. P. Rotella, B. D. Greenberg and R. Siman (1999). "Rank-order of potencies for inhibition of the secretion of abeta40 and abeta42 suggests that both are generated by a single gamma-secretase." *J Biol Chem* 274(29): 20499-20504.
- Espinoza, M., R. de Silva, D. W. Dickson and P. Davies (2008). "Differential incorporation of tau isoforms in Alzheimer's disease." *J Alzheimers Dis* 14(1): 1-16.
- Ewis, S. A. and M. S. Abdel-Rahman (1995). "Effect of metformin on glutathione and magnesium in normal and streptozotocin-induced diabetic rats." *J Appl Toxicol* 15(5): 387-390.
- Faure, P., E. Rossini, N. Wiernsperger, M. J. Richard, A. Favier and S. Halimi (1999). "An insulin sensitizer improves the free radical defense system potential and insulin sensitivity in high fructose-fed rats." *Diabetes* 48(2): 353-357.
- Faux, N. G., C. W. Ritchie, A. Gunn, A. Rembach, A. Tsatsanis, J. Bedo, J. Harrison, L. Lannfelt, K. Blennow, H. Zetterberg, M. Ingelsson, C. L. Masters, R. E. Tanzi, J. L.

- Cummings, C. M. Herd and A. I. Bush (2010). "PBT2 rapidly improves cognition in Alzheimer's Disease: additional phase II analyses." *J Alzheimers Dis* 20(2): 509-516.
- Finch, C. A. and H. Huebers (1982). "Perspectives in iron metabolism." *N Engl J Med* 306(25): 1520-1528.
- Gammoh, N. Z. and L. Rink (2017). "Zinc in Infection and Inflammation." *Nutrients* 9(6).
- Ganz, T. (2005). "Cellular iron: ferroportin is the only way out." *Cell Metab* 1(3): 155-157.
- Goedert, M. and R. Jakes (1990). "Expression of separate isoforms of human tau protein: correlation with the tau pattern in brain and effects on tubulin polymerization." *Embo j* 9(13): 4225-4230.
- Good, P. F., P. Werner, A. Hsu, C. W. Olanow and D. P. Perl (1996). "Evidence of neuronal oxidative damage in Alzheimer's disease." *Am J Pathol* 149(1): 21-28.
- Greenfield, J. P., J. Tsai, G. K. Gouras, B. Hai, G. Thinakaran, F. Checler, S. S. Sisodia, P. Greengard and H. Xu (1999). "Endoplasmic reticulum and trans-Golgi network generate distinct populations of Alzheimer beta-amyloid peptides." *Proc Natl Acad Sci U S A* 96(2): 742-747.
- Grundke-Iqbal, I., K. Iqbal, M. Quinlan, Y. C. Tung, M. S. Zaidi and H. M. Wisniewski (1986). "Microtubule-associated protein tau. A component of Alzheimer paired helical filaments." *J Biol Chem* 261(13): 6084-6089.
- Grundke-Iqbal, I., K. Iqbal, Y. C. Tung, M. Quinlan, H. M. Wisniewski and L. I. Binder (1986). "Abnormal phosphorylation of the microtubule-associated protein tau (tau) in Alzheimer cytoskeletal pathology." *Proc Natl Acad Sci U S A* 83(13): 4913-4917.
- Guo, C., T. Wang, W. Zheng, Z. Y. Shan, W. P. Teng and Z. Y. Wang (2013). "Intranasal deferoxamine reverses iron-induced memory deficits and inhibits amyloidogenic APP processing in a transgenic mouse model of Alzheimer's disease." *Neurobiol Aging* 34(2): 562-575.
- Hare, D., S. Ayton, A. Bush and P. Lei (2013). "A delicate balance: Iron metabolism and diseases of the brain." *Front Aging Neurosci* 5: 34.
- Hare, D., S. Ayton, A. Bush and P. Lei (2013). "A delicate balance: Iron metabolism and diseases of the brain." *Front Aging Neurosci* 5.
- Harkany, T., I. Abraham, W. Timmerman, G. Laskay, B. Toth, M. Sasvari, C. Konya, J. B. Sebens, J. Korf, C. Nyakas, M. Zarandi, K. Soos, B. Penke and P. G. Luiten (2000). "beta-amyloid neurotoxicity is mediated by a glutamate-triggered excitotoxic cascade in rat nucleus basalis." *Eur J Neurosci* 12(8): 2735-2745.
- Hensley, K., J. M. Carney, M. P. Mattson, M. Aksenova, M. Harris, J. F. Wu, R. A. Floyd and D. A. Butterfield (1994). "A model for beta-amyloid aggregation and neurotoxicity based on

- free radical generation by the peptide: relevance to Alzheimer disease." *Proc Natl Acad Sci U S A* 91(8): 3270-3274.
- Hentze, M. W., M. U. Muckenthaler and N. C. Andrews (2004). "Balancing acts: molecular control of mammalian iron metabolism." *Cell* 117(3): 285-297.
- Holmes, B. B. and M. I. Diamond (2014). "Prion-like properties of Tau protein: the importance of extracellular Tau as a therapeutic target." *J Biol Chem* 289(29): 19855-19861.
- Honda, K., G. Casadesus, R. B. Petersen, G. Perry and M. A. Smith (2004). "Oxidative stress and redox-active iron in Alzheimer's disease." *Ann N Y Acad Sci* 1012: 179-182.
- Ittner, L. M., Y. D. Ke, F. Delerue, M. Bi, A. Gladbach, J. van Eersel, H. Wolfing, B. C. Chieng, M. J. Christie, I. A. Napier, A. Eckert, M. Staufenbiel, E. Hardeman and J. Gotz (2010). "Dendritic function of tau mediates amyloid-beta toxicity in Alzheimer's disease mouse models." *Cell* 142(3): 387-397.
- Kaur, D., F. Yantiri, S. Rajagopalan, J. Kumar, J. Q. Mo, R. Boonplueang, V. Viswanath, R. Jacobs, L. Yang, M. F. Beal, D. DiMonte, I. Volitaskis, L. Ellerby, R. A. Cherny, A. I. Bush and J. K. Andersen (2003). "Genetic or pharmacological iron chelation prevents MPTP-induced neurotoxicity in vivo: a novel therapy for Parkinson's disease." *Neuron* 37(6): 899-909.
- King, J. C., K. H. Brown, R. S. Gibson, N. F. Krebs, N. M. Lowe, J. H. Siekmann and D. J. Raiten (2016). "Biomarkers of Nutrition for Development (BOND)—Zinc Review." *J Nutr* 146(4): 858s-885s.
- Kosik, K. S., C. L. Joachim and D. J. Selkoe (1986). "Microtubule-associated protein tau (tau) is a major antigenic component of paired helical filaments in Alzheimer disease." *Proc Natl Acad Sci U S A* 83(11): 4044-4048.
- Kruman, II, C. Culmsee, S. L. Chan, Y. Kruman, Z. Guo, L. Penix and M. P. Mattson (2000). "Homocysteine elicits a DNA damage response in neurons that promotes apoptosis and hypersensitivity to excitotoxicity." *J Neurosci* 20(18): 6920-6926.
- Lee, V. M., M. Goedert and J. Q. Trojanowski (2001). "Neurodegenerative tauopathies." *Annu Rev Neurosci* 24: 1121-1159.
- Lei, P., S. Ayton, D. I. Finkelstein, L. Spoerri, G. D. Ciccotosto, D. K. Wright, B. X. Wong, P. A. Adlard, R. A. Cherny, L. Q. Lam, B. R. Roberts, I. Volitakis, G. F. Egan, C. A. McLean, R. Cappai, J. A. Duce and A. I. Bush (2012). "Tau deficiency induces parkinsonism with dementia by impairing APP-mediated iron export." *Nat Med* 18(2): 291-295.
- Leskovjan, A. C., A. Kretlow, A. Lanzirrotti, R. Barrea, S. Vogt and L. M. Miller (2011). "Increased brain iron coincides with early plaque formation in a mouse model of Alzheimer's disease." *Neuroimage* 55(1): 32-38.

- Lipton, S. A., W. K. Kim, Y. B. Choi, S. Kumar, D. M. D'Emilia, P. V. Rayudu, D. R. Arnelle and J. S. Stamler (1997). "Neurotoxicity associated with dual actions of homocysteine at the N-methyl-D-aspartate receptor." *Proc Natl Acad Sci U S A* 94(11): 5923-5928.
- Marreiro, D. D., K. J. Cruz, J. B. Morais, J. B. Beserra, J. S. Severo and A. R. de Oliveira (2017). "Zinc and Oxidative Stress: Current Mechanisms." *Antioxidants (Basel)* 6(2).
- Meadowcroft, M. D., J. R. Connor, M. B. Smith and Q. X. Yang (2009). "MRI and histological analysis of beta-amyloid plaques in both human Alzheimer's disease and APP/PS1 transgenic mice." *J Magn Reson Imaging* 29(5): 997-1007.
- Miller, J. W. (1999). "Homocysteine and Alzheimer's disease." *Nutr Rev* 57(4): 126-129.
- Mondragon-Rodriguez, S., G. Perry, X. Zhu, P. I. Moreira, M. C. Acevedo-Aquino and S. Williams (2013). "Phosphorylation of tau protein as the link between oxidative stress, mitochondrial dysfunction, and connectivity failure: implications for Alzheimer's disease." *Oxid Med Cell Longev* 2013: 940603.
- Moos, T., T. Rosengren Nielsen, T. Skjorringe and E. H. Morgan (2007). "Iron trafficking inside the brain." *J Neurochem* 103(5): 1730-1740.
- Moreira, P. I., C. Carvalho, X. Zhu, M. A. Smith and G. Perry (2010). "Mitochondrial dysfunction is a trigger of Alzheimer's disease pathophysiology." *Biochim Biophys Acta* 1802(1): 2-10.
- Niwa, T., T. Katsuzaki, T. Momoi, T. Miyazaki, H. Ogawa, A. Saito, S. Miyazaki, K. Maeda, N. Tatemichi and Y. Takei (1996). "Modification of beta 2m with advanced glycation end products as observed in dialysis-related amyloidosis by 3-DG accumulating in uremic serum." *Kidney Int* 49(3): 861-867.
- Nordberg, A. (2008). "Amyloid plaque imaging in vivo: current achievement and future prospects." *Eur J Nucl Med Mol Imaging* 35 Suppl 1: S46-50.
- O'Brien, R. J. and P. C. Wong (2011). "Amyloid precursor protein processing and Alzheimer's disease." *Annu Rev Neurosci* 34: 185-204.
- Pavlovic, D., R. Kocic, G. Kocic, T. Jevtovic, S. Radenkovic, D. Mikic, M. Stojanovic and P. B. Djordjevic (2000). "Effect of four-week metformin treatment on plasma and erythrocyte antioxidative defense enzymes in newly diagnosed obese patients with type 2 diabetes." *Diabetes Obes Metab* 2(4): 251-256.
- Pooler, A. M., E. C. Phillips, D. H. Lau, W. Noble and D. P. Hanger (2013). "Physiological release of endogenous tau is stimulated by neuronal activity." *EMBO Rep* 14(4): 389-394.
- Qin, Y., W. Zhu, C. Zhan, L. Zhao, J. Wang, Q. Tian and W. Wang (2011). "Investigation on positive correlation of increased brain iron deposition with cognitive impairment in

- Alzheimer disease by using quantitative MR R2' mapping." *J Huazhong Univ Sci Technolog Med Sci* 31(4): 578-585.
- Qiu, C., M. Kivipelto and E. von Strauss (2009). "Epidemiology of Alzheimer's disease: occurrence, determinants, and strategies toward intervention." *Dialogues Clin Neurosci* 11(2): 111-128.
- Ridge, P. G., M. T. Ebbert and J. S. Kauwe (2013). "Genetics of Alzheimer's disease." *Biomed Res Int* 2013: 254954.
- Ritchie, C. W., A. I. Bush, A. Mackinnon, S. Macfarlane, M. Mastwyk, L. MacGregor, L. Kiers, R. Cherny, Q. X. Li, A. Tammer, D. Carrington, C. Mavros, I. Volitakis, M. Xilinas, D. Ames, S. Davis, K. Beyreuther, R. E. Tanzi and C. L. Masters (2003). "Metal-protein attenuation with iodochlorhydroxyquin (clioquinol) targeting Abeta amyloid deposition and toxicity in Alzheimer disease: a pilot phase 2 clinical trial." *Arch Neurol* 60(12): 1685-1691.
- Roberson, E. D., K. Scarce-Levie, J. J. Palop, F. Yan, I. H. Cheng, T. Wu, H. Gerstein, G. Q. Yu and L. Mucke (2007). "Reducing endogenous tau ameliorates amyloid beta-induced deficits in an Alzheimer's disease mouse model." *Science* 316(5825): 750-754.
- Shankar, G. M. and D. M. Walsh (2009). "Alzheimer's disease: synaptic dysfunction and Abeta." *Mol Neurodegener* 4: 48.
- Smith, M. A., P. L. Harris, L. M. Sayre and G. Perry (1997). "Iron accumulation in Alzheimer disease is a source of redox-generated free radicals." *Proc Natl Acad Sci U S A* 94(18): 9866-9868.
- Smith, M. A., P. L. R. Harris, L. M. Sayre and G. Perry (1997). "Iron accumulation in Alzheimer disease is a source of redox-generated free radicals." *Proc Natl Acad Sci U S A* 94(18): 9866-9868.
- Stamer, K., R. Vogel, E. Thies, E. Mandelkow and E. M. Mandelkow (2002). "Tau blocks traffic of organelles, neurofilaments, and APP vesicles in neurons and enhances oxidative stress." *J Cell Biol* 156(6): 1051-1063.
- Sultan, A., F. Nessler, M. Violet, S. Begard, A. Loyens, S. Talahari, Z. Mansuroglu, D. Marzin, N. Sergeant, S. Humez, M. Colin, E. Bonnefoy, L. Buee and M. C. Galas (2011). "Nuclear tau, a key player in neuronal DNA protection." *J Biol Chem* 286(6): 4566-4575.
- Sultana, R., M. Perluigi and D. A. Butterfield (2013). "Lipid Peroxidation Triggers Neurodegeneration: A Redox Proteomics View into the Alzheimer Disease Brain." *Free Radic Biol Med* 62: 157-169.
- Tessier, D., P. Maheux, A. Khalil and T. Fulop (1999). "Effects of gliclazide versus metformin on the clinical profile and lipid peroxidation markers in type 2 diabetes." *Metabolism* 48(7): 897-903.

- Theil, E. C. (2004). "Iron, ferritin, and nutrition." *Annu Rev Nutr* 24: 327-343.
- Todorich, B. M. and J. R. Connor (2004). "Redox metals in Alzheimer's disease." *Ann N Y Acad Sci* 1012: 171-178.
- Watt, R. K. (2013). "A unified model for ferritin iron loading by the catalytic center: implications for controlling "free iron" during oxidative stress." *Chembiochem* 14(4): 415-419.
- Weingarten, M. D., A. H. Lockwood, S. Y. Hwo and M. W. Kirschner (1975). "A protein factor essential for microtubule assembly." *Proc Natl Acad Sci U S A* 72(5): 1858-1862.
- Xu, F., S. Farkas, S. Kortbeek, F. X. Zhang, L. Chen, G. W. Zamponi and N. I. Syed (2012). "Mercury-induced toxicity of rat cortical neurons is mediated through N-methyl-D-Aspartate receptors." *Mol Brain* 5: 30.
- Yamada, K., J. K. Holth, F. Liao, F. R. Stewart, T. E. Mahan, H. Jiang, J. R. Cirrito, T. K. Patel, K. Hochgrafe, E. M. Mandelkow and D. M. Holtzman (2014). "Neuronal activity regulates extracellular tau in vivo." *J Exp Med* 211(3): 387-393.
- Younkin, S. G. (1998). "The role of A beta 42 in Alzheimer's disease." *J Physiol Paris* 92(3-4): 289-292.
- Zhou, L., B. L. Miller, C. H. McDaniel, L. Kelly, O. J. Kim and C. A. Miller (1998). "Frontotemporal dementia: neuropil spheroids and presynaptic terminal degeneration." *Ann Neurol* 44(1): 99-109.

CHAPTER 2: Hippocampal T2 Signal Loss During Aging in Transgenic Murine Modeled for AD Reflects Pathological Lesions.

Authors: Rajan D. Adhikari¹, R. Staudte¹, M. Atmojo¹, M. Mendoza², H. Wang², R. Watt³, N. Bangerter², J. Wisco^{1,4}

¹Department of Physiology and Developmental Biology, ²Department of Electrical Engineering, ³ Department of Chemistry and Biochemistry, Brigham Young University, Provo, UT.

⁴Department of Neurobiology and Anatomy, University of Utah Medical School, Salt Lake City, UT.

Corresponding Author:

Rajan D. Adhikari

Department of Physiology and Developmental Biology

Neuroscience Center

Laboratory for Translation Anatomy of Degenerative Diseases and Developmental Disorders

4005 LSB Provo, UT 84602-1231

Phone : 208-789-8550

Fax : 801-422-0004

Email: rajandeep@hotmail.com

Abstract

APP/PS1 transgenic mice overexpressing chimeric mouse/human APP-695 and mutant human presenilin 1 (PSEN1) carrying the exon-9-deleted variant (PSEN1dE9) both directed to neurons were linked to familial Alzheimer's disease. In addition, other transgenic mice overexpressing all six isoforms of hyper-phosphorylated of microtubule associated protein tau (MAPT) were scanned at various ages and compared with age controlled WT. Mean T2 turbo spin echo (TSE) signals obtained from in vivo T2 weighted MRI on these mice revealed significant signal loss in bilateral hippocampi when compared by age. There was, however, no effect of signal loss when compared to rescue treatments with or without oxidative insults. This in vivo analysis of signal loss, due to iron in the plaques, outlines a possibility to refine the imaging techniques in pursuit of a noninvasive diagnostic biomarker.

Introduction

Alzheimer's disease (AD) is a progressive neurodegenerative disorder characterized by memory loss and progressive loss of cognitive functions that impede performances in daily activities. It is mostly seen in the elderly population and is the leading cause of dementia. The diagnostic hallmarks of AD are the presence of amyloid beta plaques, neurofibrillary tangles from phosphorylated tau proteins, neurodegeneration and synapse loss (Katzman 1986, Coleman, Federoff et al. 2004) seen in post mortem brain biopsies. Formation of such plaques and tangles precedes, up to a decade or more, before any clinical symptoms appear (Morris, Storandt et al. 1996, Haroutunian, Perl et al. 1998). This describes the necessity of a sensitive biomarker for AD that not only helps in early diagnosis but also provides information regarding responses to possible treatments that retard disease progression (Knoll 1983, Anderson, Waters et al. 1988). AD is steadily affecting more patients, with a broader socioeconomic impact,

necessitating the quest for the development of more effective treatments and diagnostic tools (Growdon 1999). Neuroimaging techniques, MRI in particular, have been a widely used tool to study AD (de Leon, Golomb et al. 1993, de Leon, Bobinski et al. 2001)

We hypothesize that dysregulation of iron storage stimulates oxidative damage to neurons, which in turn promotes amyloid beta, and neurofibrillary tangles deposits. Both these proteins are found to have strong affinity iron (Bouras, Giannakopoulos et al. 1997, LeVine 1997, Zheng, Xin et al. 2009, Wan, Nie et al. 2011). There are studies showing strong association of iron with amyloid beta (Meadowcroft, Connor et al. 2009), and with neurofibrillary tangles (Good, Perl et al. 1992, Benveniste, Einstein et al. 1999). Since, these iron deposits can be visualized in magnetic resonance platform; we propose an increase in plaques and tangles in transgenic mice vs wild types that would be seen in MRI.

To study the possibility of detection of these pathological changes in mice brains, we investigated using APP/PS1 and MAPT transgenic mice together with age matched controls wild types on two-dimensional T2 weighted turbo-spin echo sequence using a 3T MRI scanner. Double transgenic APP/PS1 mice express both human Presenilin 1 and a chimeric amyloid precursor protein (APP). The humanized APP transgene allows mice to secrete a human beta peptide, and inclusion of Swedish mutation elevates the amount of amyloid beta production by favoring processing through the beta secretase pathway. The PS1 transgene expresses a mutant human presenilin 1 associated with familial AD. In these mice, amyloid plaques start depositing by six months of age (Savonenko, Xu et al. 2005). MAPT mice are homozygous for the targeted allele and hemizygous for the transgene; they express all six isoforms of human MAPT. These hyper-phosphorylated MAPT are detected in the brain by three months of age (Andorfer, Kress et al. 2003). These mice, therefore, were ideal for our experiment to scan them at one, three, six

and nine months of their age. We ran two-dimensional T2 weighted turbo-spin echo sequence to image the hippocampal signal dropouts. Our results show significant T2 signal decay in these transgenic mice as compared to age-controlled wild types.

Materials and Methods

Animals

All MRI experiments were conducted at Magnetic Resonance Imaging Research Facility, BYU-Provo. Institutional Animal Care and Use Committee (IACUC) approved MRI procedures and all animals were treated in accordance with their guidelines. 18 mice (7F, 11M) homozygous for MAPT allele and hemizygous for human MAPT transgene and the other 18 mice (10F, 8M) double transgenic for human APP and human PS1 were bred and confirmed by genotyping. Their results were compared with age matched controlled 18 wild types (4F, 14M).

Diet

All mice received ad libitum supply of regular chow purchased from Harlan Teklad (TD 8604) until one month of age. Methionine rich diet purchased from Harlan Teklad (TD 150154) was introduced to half of the mice for all strain type to trigger elevated homocysteine, while the other half continued on the same regular diet. At three months, one mouse per strain from each diet type were sacrificed and tissues harvested for experiments. Remaining eight mice per strain from each diet type were further divided into four pairs: three pairs receiving additional rescue treatment with: Metformin, Zinc or Clioquinol .A remaining pair continued on the same diet. Mice were scanned using MRI at one, three, six and nine months of age.

Anesthesia

Mice were placed in a chamber connected with a constant flow of 3-4% isoflurane in oxygen to induce anesthesia. When the mice were sufficiently induced, they were quickly transferred and placed in a prone position in a special designed table with a custom nosecone attached to a delivery system that supplied a regular flow of isoflurane mixed with oxygen. During maintenance of anesthesia, the flow was adjusted to 1L/min and concentration of isoflurane to 1.5%. This was delivered with an isoflurane vaporizer/ anesthesia machine (Veterinary Anesthesia Systems, INC.) equipped with Pureline® oxygen concentrator. Eyes were protected with an ophthalmic ointment to prevent any corneal damage. Post scanning, mice were placed in a flat bed and were continuously monitored until they could normally access food and water.

MRI Scanning

The structure scans use two-dimensional T2 weighted turbo-spin echo sequence. The sequence was implemented using a 3T Siemens whole-body scanner (Siemens Medical Systems, Erlangen, Germany) with a custom-made 4-turn Transmit/Receive (TR) solenoid radio frequency mouse coil. The FOV of the scan is 87mm (readout) x 24.5mm (phase) x 0.9mm (slice) and the acquisition matrix was 320 (readout) x 90 (phase encode) and 42 in slices direction (12 slices were used for oversample) which yields the voxel size equal to 0.27 x 0.27 x 0.9mm. Because of the small voxel size, 16 averages were employed in pursuit of a decent SNR, which made the total acquisition, time about 23 minutes. The TR/TE = 8000/115 ms, and flip angle was 150 degrees. Other acquisition parameters were turbo factor of 12, the readout bandwidth = 340 Hz/pixel. Fast mode RF pulse was selected and the slice distance was 0.45mm.

Estimation of Signal Intensities

OsiriX platform was used to calculate the signal intensities (Figure 2.1). An area of 2.001 mm² (W: 1.694 mm H: 1.504 mm P: 5.0 mm) was chosen over bilateral hippocampi as our region of interest (ROI) (Figure: 2.1). The maximum signal intensities from ROI were normalized with the intensities from the ipsilateral eye, which was used as an internal control. The average mean values were analyzed on SPSS software.

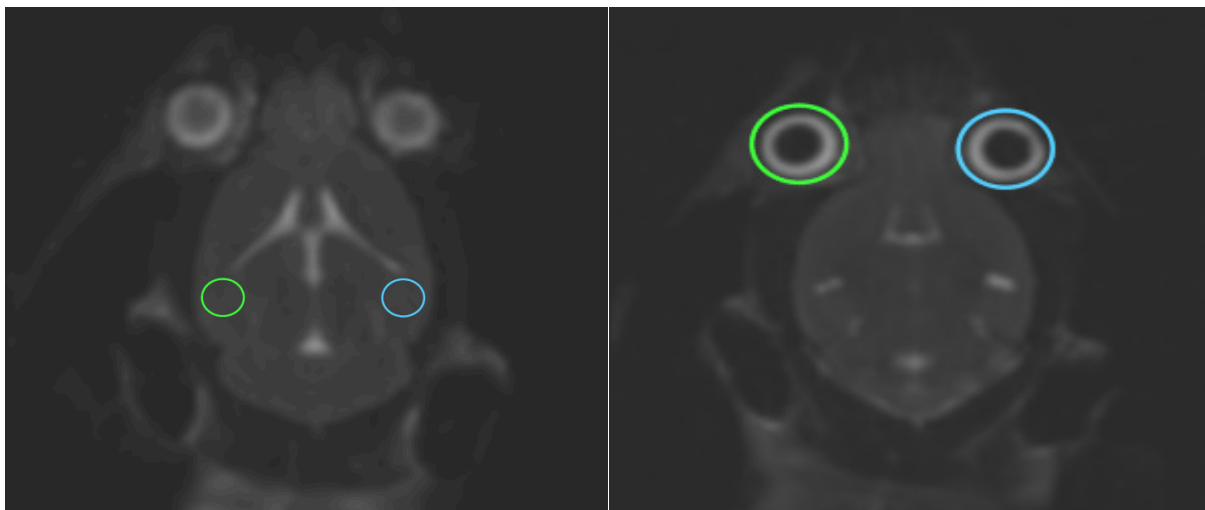


Figure 2.1: T2 weighted MRI Scan. Image constructed following 2D T2 weighted turbo spin echo sequence on mice brain at the age of one, three, six and nine months. Signal dropouts over bilateral hippocampi (Left) were measured after normalizing with maximum signal intensities from the ipsilateral eye (Right).

Results

Eighteen APP/PS1 mice, 18 Tau, and 18 WT mice were imaged and analyzed separately for the effect of time on mean T2 TSE signal. APP/PS1 [F (3, 21) =5.410, p=0.006] and Tau [F (3, 21) =11.861, p<0.001], but not WT [F (3, 21) =0.705, p=0.560] mice showed a significant signal decline with age in the left hippocampus. Likewise, APP/PS1 [F (3, 21) =4.720, p=0.011] and Tau [F (3, 21) =8.384, p=0.001], but not WT [F (3, 21) =0.493, p=0.691] mice showed a significant signal decline with age in the right hippocampus. Expected accumulation of the pathological proteins beta-amyloid and tau in the hippocampus of the respective APP/PS1 and Tau transgenic mice appeared to result in a measurable T2 signal decay compared with that of WT mice. Rescue treatments started at three months prevented further loss in T2 signals. Future studies include histological and Western blot confirmation.

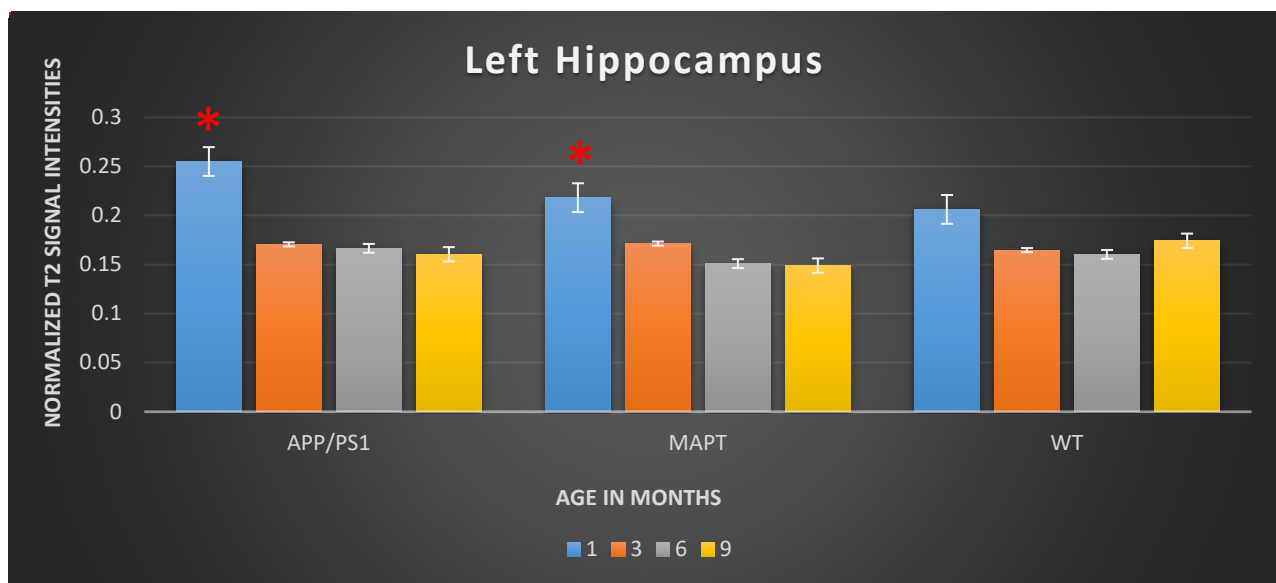


Figure 2.2: T2 Signal Intensities Over Left Hippocampus. Corresponding to the oxidative stress started at one month: an average T2 signal measured at age one month, over left hippocampus, was significantly decreased when measured again at three, six and nine months for APP/PS1 and MAPT mice but not WT. Rescue treatments were started at three months which limited the pathological changes thereafter.

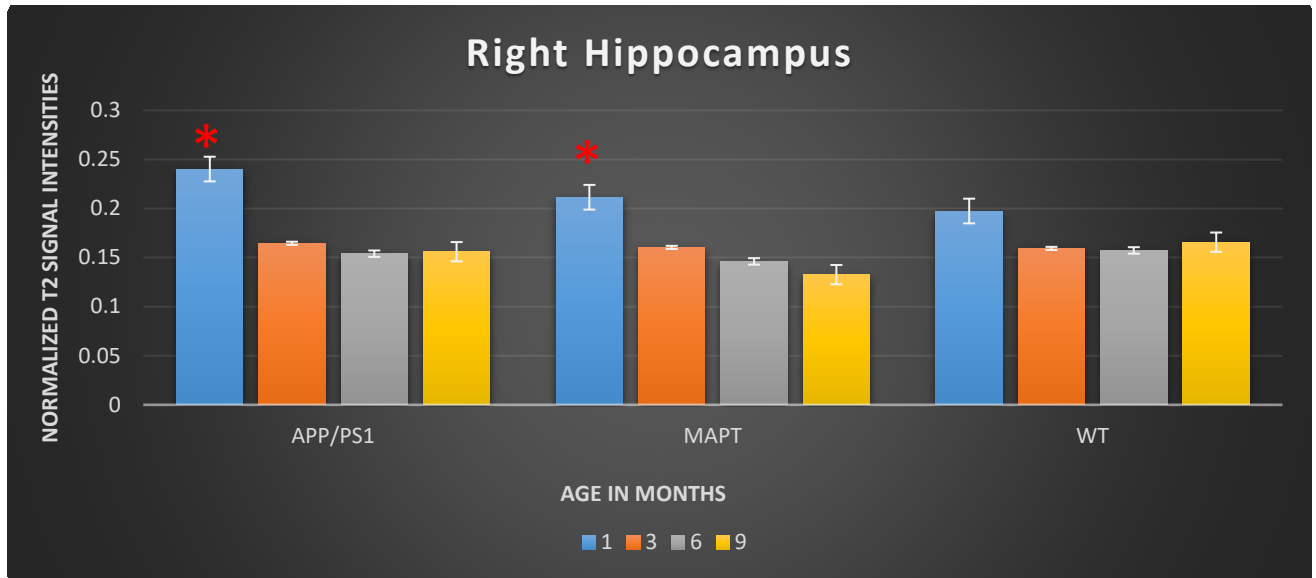


Figure 2.3: T2 Signal Intensities Over Right Hippocampus. Corresponding to the oxidative stress started at one month: an average T2 signal measured at age one month, over right hippocampus, was significantly decreased when measured again at three, six and nine months for APP/PS1 and MAPT mice but not WT. Rescue treatments were started at three months which limited the pathological changes thereafter.

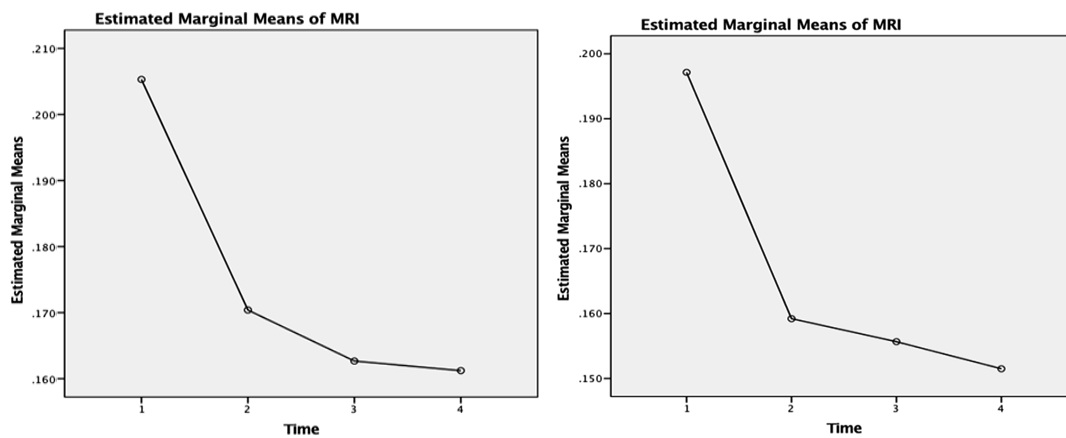


Figure 2.4: Estimated Marginal Means of MRI. Marginal means measured for bilateral hippocampus against time (1= one month, 2=three month, 3=six month and 4=nine month). Both left and right hippocampi show significant decrease in means between one and three months.

Discussion

While there have been studies showing evidence of plaques in brain tissues using 7.1 T (300 MHz) magnet (Benveniste, Einstein et al. 1999), and in mice models (Andorfer, Kress et al. 2003, Savonenko, Xu et al. 2005); usefulness of MRI in diagnosis and evaluation of AD in humans are still limited. In this present study, we have demonstrated a T2 signal decrease in bilateral hippocampi of human transgenic mice for AD. We believe that this is due to an accumulation of iron in the pathological lesions associated with the disease: amyloid beta plaques, neurofibrillary tangles or both. Presence of iron contributes T2 signal loss due to field inhomogeneity (Bizzi, Brooks et al. 1990, Vymazal, Brooks et al. 1992, Vymazal, Brooks et al. 1995), which alters the brain water content (Miot, Hoffschir et al. 1995). Figure 2.3 shows average signal intensities and figure 2.4 shows estimated marginal means measured on APP/PS1, MAPT and WT mice over one, three, six and nine months. These data show a significant drop in the mean T2 signals among transgenic mice, highest between one and three months of age suggesting early pathology. These mice were modeled to produce pathological lesion by three to six months, but with oxidative stress, they began early. With oxidative stress treatment starting at one month, neurons robustly tried to manage neuronal damage by sequestering free iron. This overwhelming process of sequestering iron is reflected by a loss of signal in hippocampi, where we expect these pathological changes to happen in abundance. By three months, when rescue treatments were started, much of the neuronal damages have already happened and were irreversible. However, mice continued to receive oxidative stress treatment throughout their life. However, the signals measured at and after three months did not have significant differences. This corresponds to effectiveness of rescue measures that prevented further damages to neurons. T2 signal changes did not return to normal, because rescue

treatments only impedes disease progression but irreversible damage that has already happened. Since, WT mice do not produce any plaques or tangles; they were able to manage oxidative insult by homocysteine, which was reflected as no significant changes in their T2 signals.

Axial 3.0T T2 weighted images, however, did not show any observable differences, between strains at different ages, with or without treatments. Iron deposits in various parts of brain have been successfully studied using T2 weighted MRI (Hallgren and Sourander 1958, Vymazal, Brooks et al. 1992) and Hallgren and Sourander have demonstrated MRI sensitivity to iron quantity in different brain regions, corresponding to qualitative MRI observation (Vymazal, Brooks et al. 1995). The amount of iron in a plaque of a mice brain is too small to be sensitive enough for it to be observed in an image. A higher magnetic field has better sensitivity for observing small quantities of iron. T2 signal decreases relative to the iron contribution linearly, dependent on the magnetic field (Vymazal, Brooks et al. 1995). Higher signal-to-noise ratios offer better image qualities with contrast features, but this comes with longer acquisition time; which makes it more difficult to scan humans, or in many cases, animal models. This suggests the limitations of our imaging techniques to visualize iron on T2 weighted images. However, our study shows a correlation between T2 weighted MRI signal and neuropathological changes in mice model for AD, especially at an early age.

Acknowledgements

The authors wish to thank the following funding sources: NIH/NIA 1 R21 AG037843; Brigham Young University, College of Life Sciences, Mentoring Environment Grant; Brigham Young University, School of Family Life, Gerontology Program; Brigham Young University, Magnetic Resonance Imaging Research Facility Seed Grant; Dr. Sarah M.

McGinty Neuroscience Graduate Student Research Fellowship; Neurodar, LLC; Limitless
Worldwide, LLC.

References

- Anderson, D. K., T. R. Waters and E. D. Means (1988). "Pretreatment with alpha tocopherol enhances neurologic recovery after experimental spinal cord compression injury." *J Neurotrauma* 5(1): 61-67.
- Andorfer, C., Y. Kress, M. Espinoza, R. de Silva, K. L. Tucker, Y. A. Barde, K. Duff and P. Davies (2003). "Hyperphosphorylation and aggregation of tau in mice expressing normal human tau isoforms." *J Neurochem* 86(3): 582-590.
- Benveniste, H., G. Einstein, K. R. Kim, C. Hulette and G. A. Johnson (1999). "Detection of neuritic plaques in Alzheimer's disease by magnetic resonance microscopy." *Proc Natl Acad Sci U S A* 96(24): 14079-14084.
- Bizzi, A., R. A. Brooks, A. Brunetti, J. M. Hill, J. R. Alger, R. S. Miletich, T. L. Francavilla and G. Di Chiro (1990). "Role of iron and ferritin in MR imaging of the brain: a study in primates at different field strengths." *Radiology* 177(1): 59-65.
- Bouras, C., P. Giannakopoulos, P. F. Good, A. Hsu, P. R. Hof and D. P. Perl (1997). "A laser microprobe mass analysis of brain aluminum and iron in dementia pugilistica: comparison with Alzheimer's disease." *Eur Neurol* 38(1): 53-58.
- Coleman, P., H. Federoff and R. Kurlan (2004). "A focus on the synapse for neuroprotection in Alzheimer disease and other dementias." *Neurology* 63(7): 1155-1162.
- de Leon, M., M. Bobinski, A. Convit, O. Wolf and R. Insausti (2001). "Usefulness of MRI measures of entorhinal cortex versus hippocampus in AD." *Neurology* 56(6): 820-821.
- de Leon, M. J., J. Golomb, A. E. George, A. Convit, C. Y. Tarshish, T. McRae, S. De Santi, G. Smith, S. H. Ferris, M. Noz and et al. (1993). "The radiologic prediction of Alzheimer disease: the atrophic hippocampal formation." *AJNR Am J Neuroradiol* 14(4): 897-906.
- Good, P. F., D. P. Perl, L. M. Bierer and J. Schmeidler (1992). "Selective accumulation of aluminum and iron in the neurofibrillary tangles of Alzheimer's disease: a laser microprobe (LAMMA) study." *Ann Neurol* 31(3): 286-292.
- Growdon, J. H. (1999). "Biomarkers of Alzheimer disease." *Arch Neurol* 56(3): 281-283.
- Hallgren, B. and P. Sourander (1958). "The effect of age on the non-haemin iron in the human brain." *J Neurochem* 3(1): 41-51.
- Haroutunian, V., D. P. Perl, D. P. Purohit, D. Marin, K. Khan, M. Lantz, K. L. Davis and R. C. Mohs (1998). "Regional distribution of neuritic plaques in the nondemented elderly and subjects with very mild Alzheimer disease." *Arch Neurol* 55(9): 1185-1191.
- Katzman, R. (1986). "Alzheimer's disease." *N Engl J Med* 314(15): 964-973.

- Knoll, J. (1983). "Deprenyl (selegiline): the history of its development and pharmacological action." *Acta Neurol Scand Suppl* 95: 57-80.
- LeVine, S. M. (1997). "Iron deposits in multiple sclerosis and Alzheimer's disease brains." *Brain Res* 760(1-2): 298-303.
- Meadowcroft, M. D., J. R. Connor, M. B. Smith and Q. X. Yang (2009). "MRI and histological analysis of beta-amyloid plaques in both human Alzheimer's disease and APP/PS1 transgenic mice." *J Magn Reson Imaging* 29(5): 997-1007.
- Miot, E., D. Hoffschir, J. L. Poncy, R. Masse, A. Le Pape and S. Akoka (1995). "Magnetic resonance imaging in vivo monitoring of T2 relaxation time: quantitative assessment of primate brain maturation." *J Med Primatol* 24(2): 87-93.
- Morris, J. C., M. Storandt, D. W. McKeel, Jr., E. H. Rubin, J. L. Price, E. A. Grant and L. Berg (1996). "Cerebral amyloid deposition and diffuse plaques in "normal" aging: Evidence for presymptomatic and very mild Alzheimer's disease." *Neurology* 46(3): 707-719.
- Savonenko, A., G. M. Xu, T. Melnikova, J. L. Morton, V. Gonzales, M. P. Wong, D. L. Price, F. Tang, A. L. Markowska and D. R. Borchelt (2005). "Episodic-like memory deficits in the APP^{swe}/PS1^{dE9} mouse model of Alzheimer's disease: relationships to beta-amyloid deposition and neurotransmitter abnormalities." *Neurobiol Dis* 18(3): 602-617.
- Vymazal, J., R. A. Brooks, N. Patronas, M. Hajek, J. W. Bulte and G. Di Chiro (1995). "Magnetic resonance imaging of brain iron in health and disease." *J Neurol Sci* 134 Suppl: 19-26.
- Vymazal, J., R. A. Brooks, O. Zak, C. McRill, C. Shen and G. Di Chiro (1992). "T1 and T2 of ferritin at different field strengths: effect on MRI." *Magn Reson Med* 27(2): 368-374.
- Wan, L., G. Nie, J. Zhang, Y. Luo, P. Zhang, Z. Zhang and B. Zhao (2011). "beta-Amyloid peptide increases levels of iron content and oxidative stress in human cell and *Caenorhabditis elegans* models of Alzheimer disease." *Free Radic Biol Med* 50(1): 122-129.
- Zheng, W., N. Xin, Z. H. Chi, B. L. Zhao, J. Zhang, J. Y. Li and Z. Y. Wang (2009). "Divalent metal transporter 1 is involved in amyloid precursor protein processing and Abeta generation." *Faseb j* 23(12): 4207-4217.

CHAPTER 3: Dual Role of Zinc: NMR Relaxometry Measurements
on Pathological and Normal Murine Brain.

Authors: Rajan D. Adhikari¹, R. Lee¹, K. Noorda¹, B. Ramfjord¹, S. Burt², R. Watt², J. Wisco^{1,4}

¹Department of Physiology and Developmental Biology, ²Department of Electrical Engineering, ³ Department of Chemistry and Biochemistry, Brigham Young University, Provo, UT.

⁴Department of Neurobiology and Anatomy, University of Utah Medical School, Salt Lake City, UT.

Corresponding Author

Rajan D. Adhikari

Department of Physiology and Developmental Biology

Neuroscience Center

Laboratory for Translation Anatomy of Degenerative Diseases and Developmental Disorders

4005 LSB Provo, UT 84602-1231

Phone: 208-789-8550

Fax: 801-422-0004

Email: rajandeep@hotmail.com

Abstract

Ultra-centrifuged brain samples were investigated with ^1H NMR Relaxometry inversion recovery and Carr-Purcell-Meiboom-Gill pulse sequences. Depending on the rescue treatment, age and strain type, we found significant decrease in T2 NMR signal in mice with no oxidative insult followed by rescue with either a normal diet or a diet rich in zinc. T2 signals were significantly low at six months of age as compared to three and nine month. WT mice showed a significant decrease in signal compared to APP/PS1 and MAPT mice. This study provides evidence of zinc in either promoting neurodegeneration in otherwise healthy neurons or protecting neurons from further oxidative damage when diseased.

Introduction

Alzheimer's disease is a major cause of dementia in the elderly population. Pathological proteins like amyloid plaques and neurofibrillary tangles are considered hallmarks for this disease (Harman 2006). In addition, these lesions precede clinical diagnosis by decades. It is still unclear what triggers these changes, and if their production are related to each other. Our hypothesis is that the free iron mediated oxidative stress induces amyloid beta plaques, to limit the excess iron. With continued oxidative stress, the plaques ultimately become exhausted. To compensate this burden, tau proteins get hyper-phosphorylated into neurofibrillary tangles and hold the free iron. Thus, we believe that the correlation between iron and these proteins changes according to the age of mice. Association of iron with amyloid beta (Falangola, Lee et al. 2005) and neurofibrillary tangles (Smith, Harris et al. 1997) has been studied in various platforms including MRI. However, optimal imaging strategies to image human are not yet available. We wanted to study the intrinsic magnetic resonance parameters, such as longitudinal (T1) and transverse (T2) relaxations times and use them to refine imaging techniques. Since, these

parameters are sensitive to changes in the biophysical environment of water; we hypothesized that the association of iron with amyloid beta and neurofibrillary tangles will have an effect on these parameters. Though, zinc is known for its antioxidant and protective role, it can be neurotoxic when a particular threshold is reached. In this study, we found evidence of zinc promoting neurodegeneration in otherwise healthy brains and protecting against oxidative damage in pathological brains.

Materials and Methods

All mice were treated ethically according to the guidelines of Institutional Animal Care and Use Committee (IACUC). These guidelines include minimizing animal suffering and the number of animals used to perform the required experiments. Mice were housed in the specific pathogen free environment at Life Science Building, BYU Provo, UT. Mice were placed in a small shoebox type cages with *Ad Libitum* access to food and water. They received normal 12hr light/dark cycle lighting. Eighteen mice each with human transgene APP/PS1 and MAPT were studied and compared with 18 other age matched wild types controls. Animals were anesthetized using isoflurane and decapitated. The brain was rapidly removed and dissected along the sagittal plane into two equal hemispheres. One hemisphere was fixed by submerging in 4% formaldehyde solution and the other hemisphere was immediately immersed into liquid nitrogen to flash freeze and then stored in -80 freezer until further use.

Frozen brain samples were weighed and freshly prepared cold tris-buffered saline solution (TBS) containing 20 mM Tris-HCl, 150 mM NaCl, pH 7.4 was added at 4: 1 v/w ratio. Protease inhibitor was added to the mixture to prevent unwanted degradation of proteins. The mixture was then homogenized at 4M/s for one minute in a MP Biomedical Fast prep 24 Homogenizer at Dr. Price's lab, BYU Provo, UT. The homogenate was transferred to 5*41 mm

ultra-clear centrifuge tubes and loaded onto sw55 Ti rotor. This setup was then ultra-centrifuged at 40,000 k rpm in a Beckman optima le- 80K Ultracentrifuge at 4-degree temperature for one hour. The supernatant was then collected and stored in -80 freezer until further use.

Hundred ul mice brain ultra-centrifuged samples were mixed with 800 ul of 99.9 % Deuterium oxide (D₂O). The mixture were then transferred into 300 MHz 5mm Ultra Precision NMR TubesTM, and stored in -20 freezer until used. NMR study was done at the Nuclear Magnetic Resonance facility in the Benson building, BYU Provo, UT. We used a Varian INOVA 300 MHz system to acquire ¹H spectra that is run by Agilent's Vnmrj 4.2 software. The NMR probe was stabilized at five °C by supplying nitrogen air passed through a heat exchanger immersed in a mixture of dry ice and isopropyl alcohol.

Inverse Recovery (T1)/Longitudinal Relaxation

For each sample, 10 inversion recovery data sets were collected. Each data set consisted of a 180° pulse, followed by a variable relaxation delay, followed by a 90° pulse, followed by a free induction decay (FID) with a total accumulation time of around 0.2 h. Each FID was a sum of four scans with a relaxation delay of 16 s before the initial 180° pulse. The FIDs were typically collected as 8192 complex data points during an acquisition period of 1.707 s. The spectral width was set at 0.0 to 9.6 ppm and the receiver gain at 30 dB. The 90o pulse widths were calibrated at 9.0 ± 0.3 us at 58 dB power. All FIDs were exponential weighted and transformed with the size of 64k, with 2 Hz of line broadening.

The VnmrJ software fit each peak in the spectrum with an exponential curve to extract the longitudinal relaxation time (T1) for each peak in the spectrum.

CPMG (T2)/Spin-Spin Relaxation

For each sample, 10 CPMG data sets were collected. Each data set consisted of a variable length train of 180° pulses with the CPMG phase alternation followed by a free induction decay (FID) with a total accumulation time of around 0.2 h. Each FID was a sum of four scans with a relaxation delay of 15 s before the train of 180° pulses. The FID was typically collected as 8192 complex data points during an acquisition period of 1.707 s. The spectra width was set at 0.0 to 9.6 ppm with a spectral width of 4799.6 Hz and the receiver gain at 30 dB. The 90° excitation pulse width was calibrated at 9.0 ± 0.3 us at 58 dB power. FID was exponentially weighted and transformed with the size of 64k, with 2 Hz of line broadening. The VnmrJ software fit each peak in the spectrum with an exponential curve to extract the spin-spin relaxation time (T2) for each peak in the spectrum.

Results

Brain homogenate from seventeen APP/PS1 mice, 18 Tau, and 18 WT mice was analyzed separately for their relaxation properties on 300 MHz NMR system. Rescue treatment had a significant effect on T2 measurements [F (8, 3) =22.888, P=0.013]. There was statistical significance either with no treatment ($p < 0.013$) or with Zinc ($p < 0.042$) as rescue measures on mice who did not receive any oxidative insult. Likewise, there was a significance difference in T2 measurements between three and six months of age ($p = 0.038$) and between six and nine months of age ($p = 0.042$), but the main effect of age on T2 measurement was trending towards significance (F [2, 3] =9.186, $p = 0.053$). Similarly, there was significant difference in T2 measurements of APP/PS1 with WT ($p = 0.025$), but not with tau ($p = 0.139$) and between WT and Tau ($p = 0.116$). The overall comparison, however was also trending towards significance [F (2,

3) =8.695, P=0.056]. However, there was no effect on T1 measurement with rescue treatments [F (8, 3) =1.352, p=0.442], age [F (2, 3) =0.605, p=0.601] and between cohorts [F (2, 3) =0.301, p=0.760].

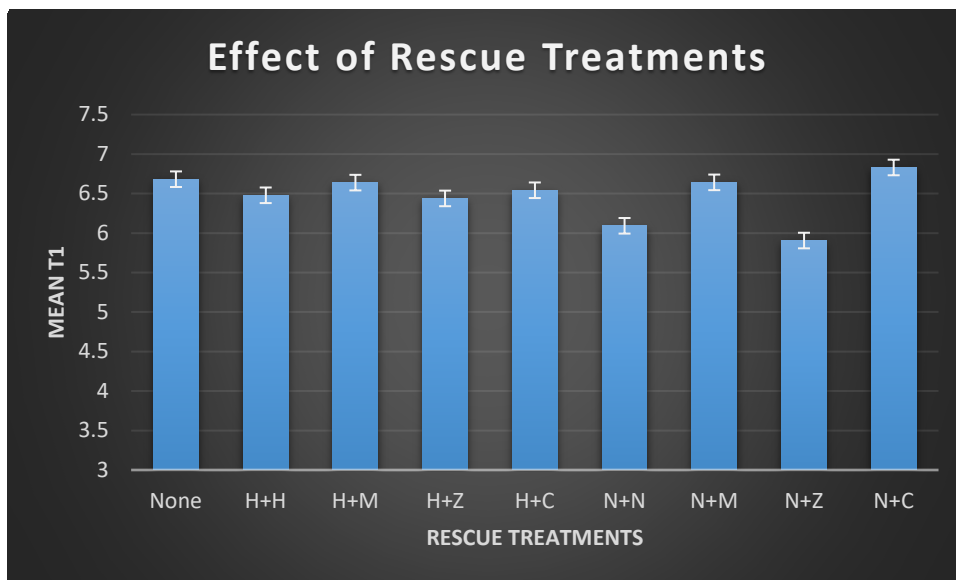


Figure 3.1: Effect of Rescue Treatments on Mean T1.NMR measurements on brain homogenates of mice that received rescue treatments with: None=No treatment, M=Metformin, Z=Zinc and C=Clioquinol, who were previously stimulated with H=Homocysteine or N=Normal Diet. T1 measurement was not significantly affected by rescue treatments (P=0.760).

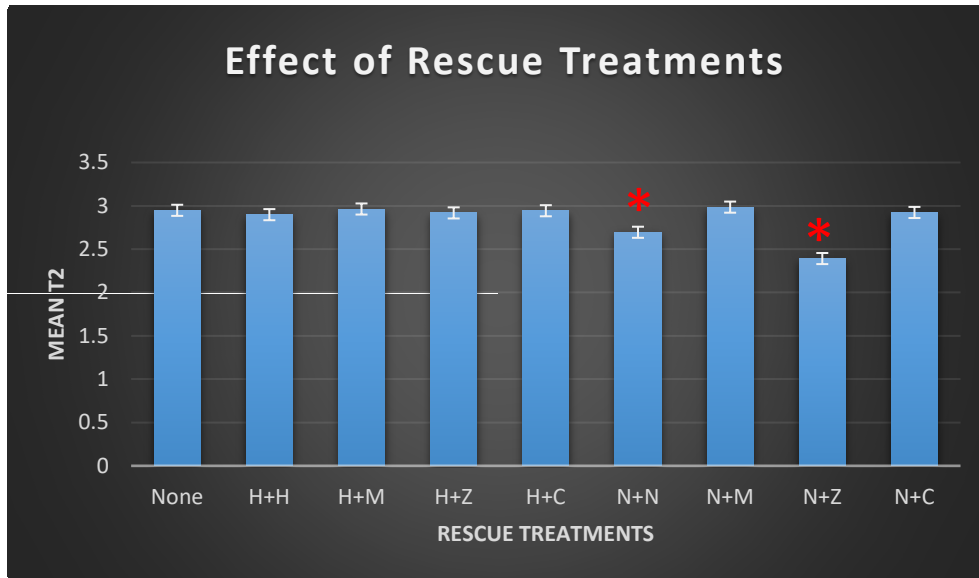


Figure 3.2: Effect of Rescue Treatments on Mean T2.NMR measurements on brain homogenates of mice that received rescue treatments with: None=No treatment, M=Metformin, Z=Zinc and C=Clioquinol, who were previously stimulated with H=Homocysteine or N=Normal Diet. Significant drop in T2 measurements were found on mice who were not stimulated by oxidative stress, but were rescued either with normal diet ($P < 0.013$) or with zinc ($P < 0.042$).

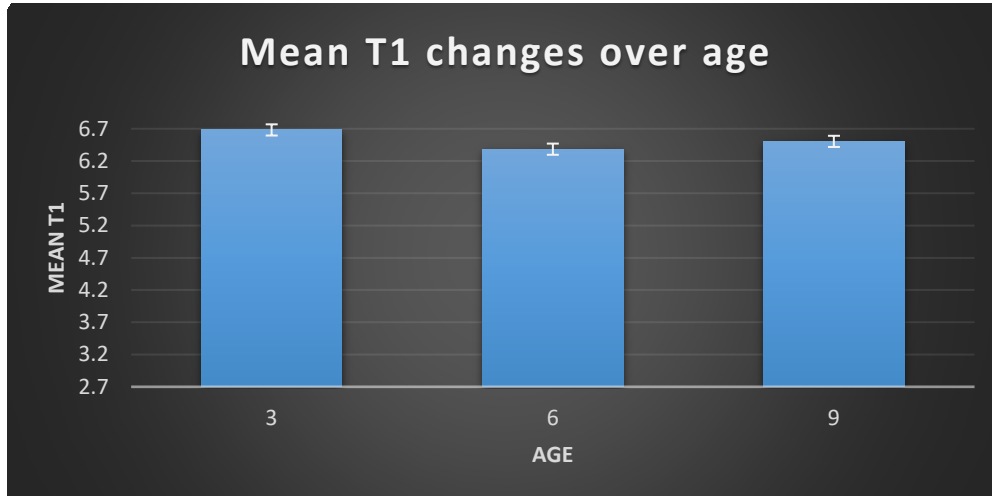


Figure 3.3: Age Effect on Mean T1. NMR measurements show no significant difference in mean T1 time, measured at the age of three, six and nine months.

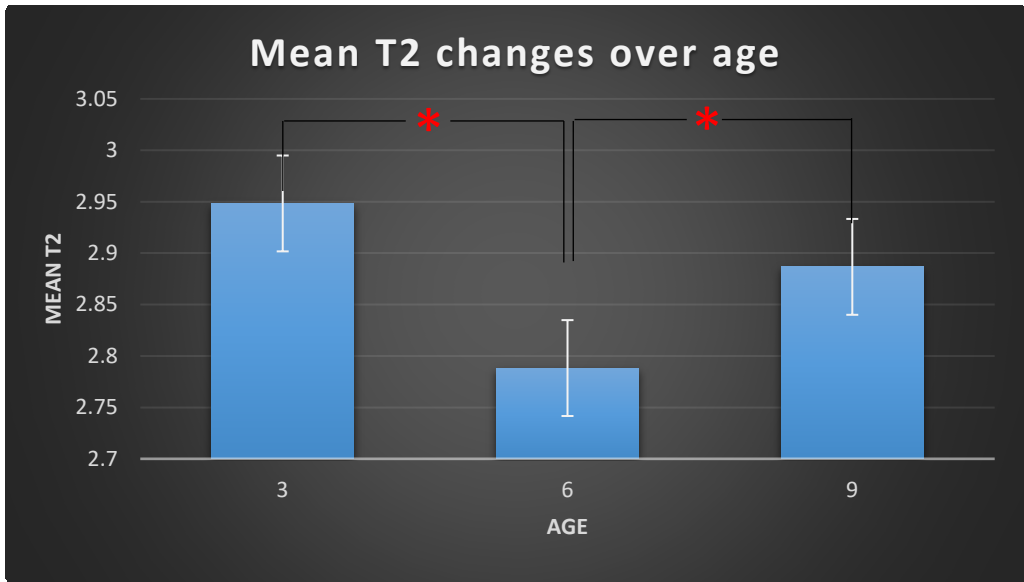


Figure 3.4: Age effect on Mean T1 and T2: NMR measurements show a significant difference in T2 time. Significance was noted between three and six months and between six and nine months.

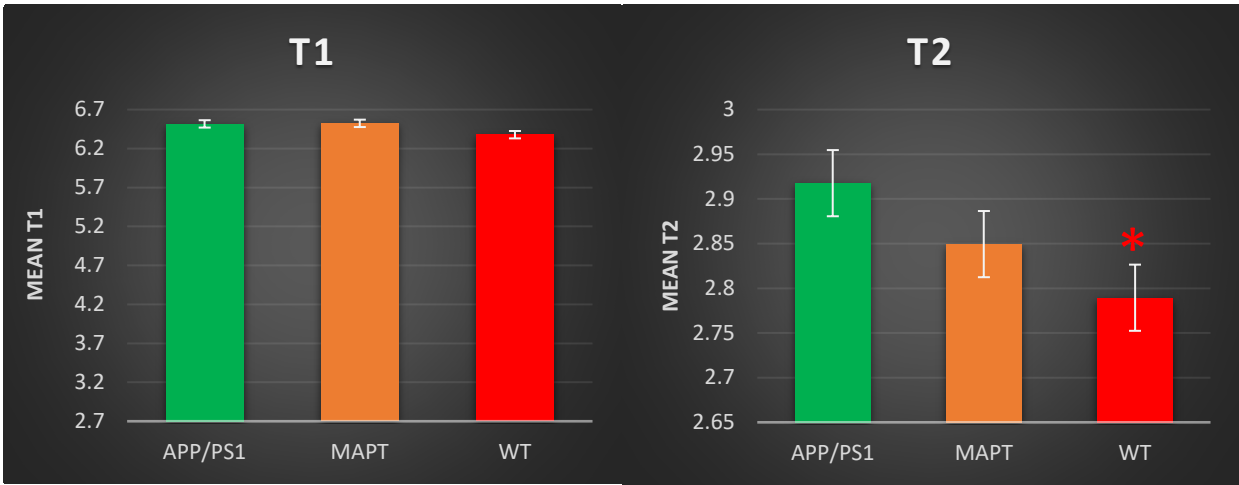


Figure 3.5: Mean T1 and T2 Effect on Strain: Only T2 measurement showed significant difference in mean T2 measurement on WT. There was no significance in T2 measurement between APP/PS1 and MAPT mice. T1 time did not show any significant changes among any strain types.

Discussion

In this present pilot study, we examined the relaxation properties of brain homogenates with varying degrees of iron related pathology. While we did not observe any significant differences in T1 values, T2 measurements were significantly affected by rescue treatments (Figure 3.1). The main significant decrease in T2 signal was found in those mice who did not receive any rescue treatment and those who received zinc as rescue. These findings were in contrast with our hypothesis. Measurements of T2 are affected by various factors, including but not limited to, sample inhomogeneity, temperature gradients across sample and paramagnetic impurities. While we do not expect any paramagnetic impurities in our sample, other than those already present, our biggest concern was sample inhomogeneity. Though we only used supernatant from brain ultracentrifuge, we do not rule out any possibility of transferring some cellular debris. Poor mixing of such solutions and presence of solid particles might have interfered with our relaxation measurement. Our experiments were conducted in a temperature-controlled environment to prevent protein denaturation. Different temperature gradients across samples, leading to convection (Loening and Keeler 1999) might have interfered in our finding. However, we do not solely attribute this finding to sample preparation and instrumentation errors. We expected zinc to reduce iron load in the lesions and increase transverse relaxation time. We believe that this is due to the amount of zinc that was given in the diet. While zinc is considered a powerful antioxidant and is known to reduce amyloid beta plaques (Cardoso, Rego et al. 2005, Garai, Sengupta et al. 2006), it can also aggregate amyloid beta at higher concentrations (Bush, Pettingell et al. 1994, Bush 2003) favoring α helical structures in A β peptides promoting aggregation (Huang, Atwood et al. 1997). We have found that around 200-300 mg of zinc per kg chow was successfully used in various studies (Simon and Taylor 2001,

Summers, Rofe et al. 2009). We followed the methods of Summers and supplemented mice diet with 200 mg zinc per kg of chow. Such studies required diets to be given for just a few months; however, we continued to feed our mice with zinc diet for nine months. We believe that this prolonged exposure to zinc might have accumulated and contributed to increase neuropathological burden: corresponding to decrease in T2 time. Similar studies have reported that addition of zinc to solution containing amyloid beta, reduces signal intensity in dual NMR experiments involving ^1H - ^{15}N and ^1H - ^{13}C (Danielsson, Pierattelli et al. 2007), primarily by binding with the histidines ligands. Zinc is also known to inhibit the ferroxidase activity of APP, increased cytosolic iron and subsequent Ab burden (Duce, Tsatsanis et al. 2010). This indicates use of Clioquinol, a powerful zinc chelator, as a therapeutic measure to lessen amyloid plaques burden and were seen effective in preclinical APP transgenic models of AD (Cherny, Atwood et al. 2001). Amount of iron present in samples with other treatments might have been too small for NMR to detect the differences. However, significant difference in T2 NMR signal between three and six months and between six and nine-month can be explained otherwise. Rescue treatment was not started until month three. When there were no or very little oxidative stressors, amount of zinc added was toxic: which explains the likelihood of zinc induced neurodegeneration, iron sequestration and T2 signal loss

Acknowledgements

The authors wish to thank the following funding sources: NIH/NIA 1 R21 AG037843; Brigham Young University, College of Life Sciences, Mentoring Environment Grant; Brigham Young University, School of Family Life, Gerontology Program; Brigham Young University, Magnetic Resonance Imaging Research Facility Seed Grant; Dr. Sarah M.

McGinty Neuroscience Graduate Student Research Fellowship; Neurodar, LLC; Limitless
Worldwide, LLC.

References

- Bush, A. I. (2003). "Copper, zinc, and the metallobiology of Alzheimer disease." *Alzheimer Dis Assoc Disord* 17(3): 147-150.
- Bush, A. I., W. H. Pettingell, G. Multhaup, M. d Paradis, J. P. Vonsattel, J. F. Gusella, K. Beyreuther, C. L. Masters and R. E. Tanzi (1994). "Rapid induction of Alzheimer A beta amyloid formation by zinc." *Science* 265(5177): 1464-1467.
- Cardoso, S. M., A. C. Rego, C. Pereira and C. R. Oliveira (2005). "Protective effect of zinc on amyloid-beta 25-35 and 1-40 mediated toxicity." *Neurotox Res* 7(4): 273-281.
- Cherny, R. A., C. S. Atwood, M. E. Xilinas, D. N. Gray, W. D. Jones, C. A. McLean, K. J. Barnham, I. Volitakis, F. W. Fraser, Y. Kim, X. Huang, L. E. Goldstein, R. D. Moir, J. T. Lim, K. Beyreuther, H. Zheng, R. E. Tanzi, C. L. Masters and A. I. Bush (2001). "Treatment with a copper-zinc chelator markedly and rapidly inhibits beta-amyloid accumulation in Alzheimer's disease transgenic mice." *Neuron* 30(3): 665-676.
- Danielsson, J., R. Pierattelli, L. Banci and A. Graslund (2007). "High-resolution NMR studies of the zinc-binding site of the Alzheimer's amyloid beta-peptide." *Febs j* 274(1): 46-59.
- Duce, J. A., A. Tsatsanis, M. A. Cater, S. A. James, E. Robb, K. Wikke, S. L. Leong, K. Perez, T. Johanssen, M. A. Greenough, H. H. Cho, D. Galatis, R. D. Moir, C. L. Masters, C. McLean, R. E. Tanzi, R. Cappai, K. J. Barnham, G. D. Ciccotosto, J. T. Rogers and A. I. Bush (2010). "Iron-export ferroxidase activity of beta-amyloid precursor protein is inhibited by zinc in Alzheimer's disease." *Cell* 142(6): 857-867.
- Falangola, M. F., S. P. Lee, R. A. Nixon, K. Duff and J. A. Helpert (2005). "Histological colocalization of iron in Abeta plaques of PS/APP transgenic mice." *Neurochem Res* 30(2): 201-205.
- Garai, K., P. Sengupta, B. Sahoo and S. Maiti (2006). "Selective destabilization of soluble amyloid beta oligomers by divalent metal ions." *Biochem Biophys Res Commun* 345(1): 210-215.
- Harman, D. (2006). "Alzheimer's disease pathogenesis: role of aging." *Ann N Y Acad Sci* 1067: 454-460.
- Huang, X., C. S. Atwood, R. D. Moir, M. A. Hartshorn, J. P. Vonsattel, R. E. Tanzi and A. I. Bush (1997). "Zinc-induced Alzheimer's Abeta1-40 aggregation is mediated by conformational factors." *J Biol Chem* 272(42): 26464-26470.
- Loening, N. M. and J. Keeler (1999). "Measurement of convection and temperature profiles in liquid samples." *J Magn Reson* 139(2): 334-341.
- Simon, S. F. and C. G. Taylor (2001). "Dietary zinc supplementation attenuates hyperglycemia in db/db mice." *Exp Biol Med* (Maywood) 226(1): 43-51.

Smith, M. A., P. L. Harris, L. M. Sayre and G. Perry (1997). "Iron accumulation in Alzheimer disease is a source of redox-generated free radicals." *Proc Natl Acad Sci U S A* 94(18): 9866-9868.

Summers, B. L., A. M. Rofe and P. Coyle (2009). "Dietary zinc supplementation throughout pregnancy protects against fetal dysmorphology and improves postnatal survival after prenatal ethanol exposure in mice." *Alcohol Clin Exp Res* 33(4): 591-600.

CHAPTER 4: Strain Specific Regulation of Proteins: An Iron Hypothesis for Alzheimer's Disease.

Authors: Rajan D. Adhikari¹, R. Watt³, N. Bangerter², S. Burt³, J. Wisco^{1, 4}

¹Department of Physiology and Developmental Biology, ²Department of Electrical Engineering, ³ Department of Chemistry and Biochemistry, Brigham Young University, Provo, UT.

⁴Department of Neurobiology and Anatomy, University of Utah Medical School, Salt Lake City, UT.

Corresponding Author:

Rajan D. Adhikari

Department of Physiology and Developmental Biology

Neuroscience Center

Laboratory for Translation Anatomy of Degenerative Diseases and Developmental Disorders

4005 LSB Provo, UT 84602-1231

Phone: 208-789-8550

Fax: 801-422-0004

Email: rajandeep@hotmail.com

Abstract

Free iron mediated oxidative stress seems to be a cornerstone in pathogenesis and progression of Alzheimer's disease (AD), which disrupts normal regulation of proteins. Ferritin upregulates to store overwhelmingly free iron, along with Ferroportin and Amyloid precursor protein promoting and shuttling out amyloid beta plaques. Tau protein gets hyperphosphorylated and aggregates into neurofibrillary tangles. We report that different strains regulate these proteins differently, but in accordance to our iron hypothesis. However, the expression of tau isoform in pathogenesis was not uniform and was found to be strain dependent, their role justified our model. Further investigations including amyloid beta and histopathological confirmation may bridge our understanding in pathogenesis of AD.

Introduction

Alzheimer's disease (AD) is a progressive neurodegenerative condition, primarily seen in the elderly population, characterized by memory loss, personality change and decline in cognitive function (Selkoe 2001). The diagnostic hallmarks of AD are presence of extracellular amyloid beta (A β) plaques and intracellular neurofibrillary tangles, which are associated with neuronal loss, astrocytosis and microglial oxidative damage (Reddy and Beal 2005, Tanzi and Bertram 2005, Reddy and McWeeney 2006). Many recent publications have attributed oxidative stress to be a major factor promoting AD progression. Due to its huge oxygen consumption, the respiratory chain in the mitochondria is vulnerable in producing superoxide, a primary reactive oxygen species (ROS)(Adam-Vizi 2005), which under normal physiological conditions, is neutralized by naturally occurring anti-oxidants. During pathological conditions in older brains, the mechanism of maintaining steady state is disrupted favoring numerous factors promoting neurodegeneration. Processing of Amyloid Precursor Protein (APP) is one such mechanisms that

get dysregulated, forming amyloid beta (A β) plaques. APP is a heterogeneous group of polypeptides, that is expressed everywhere, having a molecular weight of 110-140 kDa (Selkoe, Podlisny et al. 1988). Normally APP is cleaved by A and G secretase, but in a pathological brain, APP is aberrantly cleaved by BACE and G secretase (Haass, Schlossmacher et al. 1992, Shoji, Golde et al. 1992), producing AB. The role of AB still is an unresolved topic for debate. Some argue about AB facilitating the generation of free radicals (Behl, Davis et al. 1994, Hensley, Carney et al. 1994, Mattson 1995), while other suggest that oxidative stress precedes AB formation (Yan, Yan et al. 1995, Nunomura, Perry et al. 2000, Pratico, Uryu et al. 2001) and that AB in fact, acts as superoxide dismutase to reduce oxidative stress (Bush, Atwood et al. 2000). The expression of APP and AB are upregulated in AD brains associated with increased AB deposits (Menendez-Gonzalez, Perez-Pinera et al. 2005). Elemental iron is a potential source for hydroxyl radical that may promote oxidative damage and neurodegeneration, and there have been studies in AD brains showing altered metabolism of iron, including transferrin and ferritin, an iron transport and storage protein, respectively (Connor, Menzies et al. 1992, Good, Perl et al. 1992). Almost all iron exchange and transport is mediated by transferrin (Finch and Huebers 1982). Intracellularly, iron can follow many different pathways depending on its need. Excess iron is stored in an abundant protein called ferritin (Theil 2004). Fe²⁺ ions from the cytosol are oxidized by ferroxidase and exported into the interstitium by Ferroportin (Aisen, Enns et al. 2001). Despite lacking ferroxidase activity, APP in the neurons, interacts with Ferroportin to export iron from neurons (Wong, Tsatsanis et al. 2014) preventing oxidative damage.

We examined the expression of these AD associate proteins in mice with human transgenes for APP/PS1 and MAPT. A subset of mice from each strain was fed a methionine

rich diet to induce oxidative stress and subsequently rescued with metformin, zinc and clioquinol. Their outcomes were compared with age matched wild type controls.

Materials and Methods

Animals were anesthetized using isoflurane and decapitated. Brain rapidly removed and dissected along the sagittal plane into two equal hemispheres. One hemisphere was fixed by submerging in 4% formaldehyde solution and the other hemisphere was immediately immersed into liquid nitrogen to flash frozen and stored in -80 freezer until further use.

Frozen brain samples were weighed and freshly prepared cold tris-buffered saline solution (TBS) containing 20 mM Tris-HCl, 150 mM NaCl, pH 7.4 and Protease inhibitor was added at 4: 1 v/w ratio. The mixture was then homogenized at 4M/s for one minute in a MP Biomedical Fast prep 24 Homogenizer at Dr. Price's lab, BYU Provo, UT. The homogenate was then transferred to 5*41 mm ultra-clear centrifuge tubes and loaded onto sw55 Ti rotor. This setup was ultra-centrifuged at 40,000 rpm in a Beckman optima le- 80K Ultracentrifuge at 4-degree temperature for one hour, housed at Life Science Building, BYU Provo, UT. The supernatant was then collected and stored in -80 freezer until further use.

Protein concentration was determined using the BCA protein determination kit (Pierce). Samples were then appropriately diluted with above-mentioned TBS buffer to a uniform protein concentration of 2ug/ul across all samples. Before loading, these samples were diluted in 2x Laemmli Sample Buffer (Bio Rad) containing 1x concentration of 2.5% 2-mercaptoethanol (BME, 355mM) (gibco, Life Technologies). Final concentration of proteins in each samples, following such dilution, was 1ug/ul. Samples were boiled at 95° for 5 minutes to reduce and denature the proteins. The Criterion™ TGX™ (Tris-Glycine extended) precast gels of 4-15% gel percentage (Bio Rad) were used to load the gels. Spectra™ Multicolor Broad Range Protein

Ladder (ThermoFischer Scientific) and Precision plus Protein™ Dual Color Standards (Bio Rad) was used as a molecular weight marker. Gels were run at a constant voltage of 200 mv for 42 minutes with running buffer containing 25 mM Tris, 192 mM glycine, 0.1% SDS, pH 8.3. Tank transfer method was implemented to transfer proteins into 45um nitrocellulose membrane (Bio Rad), using a constant voltage of 100 mv for 60 minutes. Transfer buffer contained 25 mM Tris, 192 mM glycine and 20% methanol. Membranes were blocked overnight using 5% non-fat dairy milk or 5% Bovine Serum Albumin (Biomatik). Membranes were cut at appropriate positions and incubated with respective primary antibodies: 1: Rabbit Anti-phospho-MAPT (Sigma) 2: Rabbit Anti-Ferritin (Abcam) 3: Rabbit Anti-SLC40A1 (ThermoFischer Scientific) 4: Rabbit Anti-Amyloid Precursor Protein (Cell Signaling) 5: Rabbit Anti- GAPDH (Cell Signaling) and 6: Rabbit Anti-B-amyloid (Cell Signaling). GAPDH was used as a loading control. IRDye® 800CW Donkey Anti-Rabbit IgG (H+L) (LI-COR) was used as a secondary antibody.

Results

Ferritin

Brain homogenate from 17 APP/PS1 mice, 18 Tau, and 18 WT mice was analyzed separately for the expression of different proteins associated with AD. Using a univariate analysis of variance, we found a significant main effect of cohort alone on the expression of ferritin [F (2, 53) =62.539, P=0.016]. Age [F (2, 53) =0.005, P=0.995] and rescue treatment alone [F (8, 53) =0.469, P=0.819], were not significant factors. We did not find any significant main effect interaction between cohort and rescue [F (14, 53) =0.351, P=0.909], cohort and age [F (2, 53) =0.056, P=0.947], age and rescue [F (9, 53) =0.316, P=0.909], and between all three factors [F (11, 53) =0.209, P=0.968]. After adjusting for multiple comparisons using Tukey HSD analysis, we found significant difference in the expression of ferritin between APP/PS1

and WT (P=0.040) and APP/PS1 and MAPT (P=0.013) but not between WT and MAPT (P=0.066).

Tau isoforms

Using a generalized linear model, we found a significant main effect of cohort alone on the expression of tau isoforms [F (4, 53) =30.316, P=0.032] Wilk's Lambda=0.000]. None of the other factors were significant. We found significant main effect interactions between cohort and tau isoform 48 [F (2, 53) =101.146, P=0.010], cohort and tau isoform 45 [F (2, 53) =44.970, P=0.022], and cohort and tau isoform 42 [F (2, 53) =52.590, P=0.019]. After adjusting for multiple comparisons using Tukey HSD analysis, we found significant difference in the expression of tau 48 isoform between WT and APP/PS1 (P=0.007) and APP/PS1 and tau (P=0.015) but not between WT and tau (P=0.062). Likewise, expression of tau isoform 45 was significant between tau and WT (P=0.039) and tau and APP/PS1 (P=0.015), but not between APP/PS1 and WT (P=0.094). Similarly, we found significant difference in the expression of tau 42 isoform between WT and APP/PS1 (P=0.013) and between WT and tau (P=0.025) but not between APP/PS1 and tau ((P=0.149).

Tau Isoforms, Ferroportin and APP

Using a generalized linear model, we found a significant main effect of cohort alone on the expression of tau isoforms (48, 45 & 42), ferroportin and APP [F (4, 53) =18.764, P=0.051, Wilk's Lambda=0.001]. None of the other factors were significant. We found significant main effect interactions between cohort and ferroportin [F (2, 53) =24.805, P=0.039], and cohort and APP [F (2, 53) =66.248, P=0.015]. After adjusting for multiple comparisons using Tukey HSD analysis, we found significant difference in the expression of Ferroportin between WT and tau (P=0.043) and APP/PS1 and tau (P=0.043) but not between WT and APP/PS1 (P=0.993).

Likewise, expression of APP was significant between APP/PS1 and WT ($P=0.012$) and tau and APP/PS1 ($P=0.020$), but not between tau and WT ($P=0.167$).

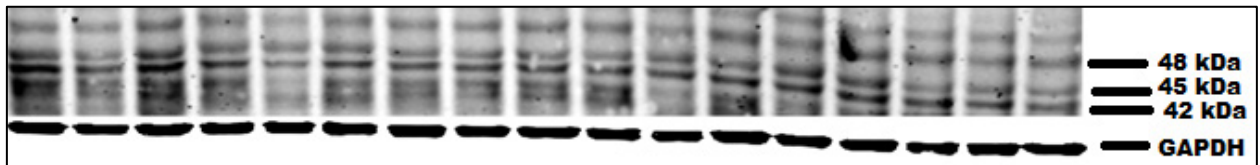


Figure 4.1: APP/PS1 and Tau Isoforms. Ultra-centrifuged brain homogenate extract were separated by SDS PAGE and probed with MAPT antibodies as described in Methods. Expression of tau isoforms (42, 45, 48) in APP/PS1 mice, density normalized to GAPDH.

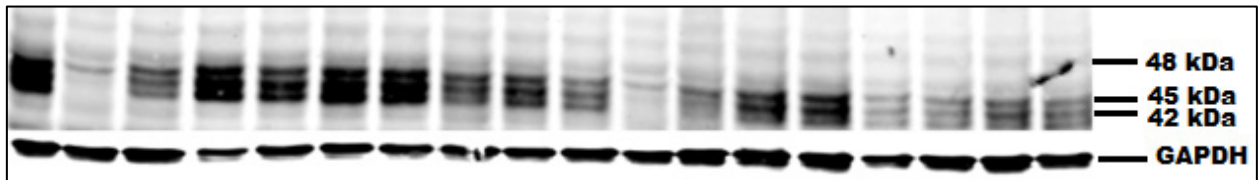


Figure 4.2: MAPT and Tau Isoforms. Ultra-centrifuged brain homogenate extract were separated by SDS PAGE and probed with MAPT antibodies as described in Methods. Expression of tau isoforms (42, 45, 48) in MAPT mice, density normalized to GAPDH.

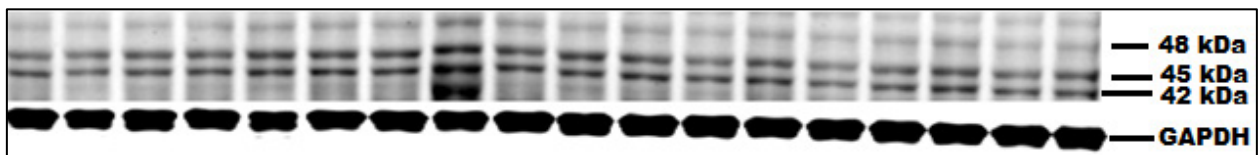


Figure 4.3: WT and Tau Isoforms. Ultra-centrifuged brain homogenate extract were separated by SDS PAGE and probed with MAPT antibodies as described in Methods. , Expression of tau isoforms (42, 45,48) in WT mice, density normalized to GAPDH.

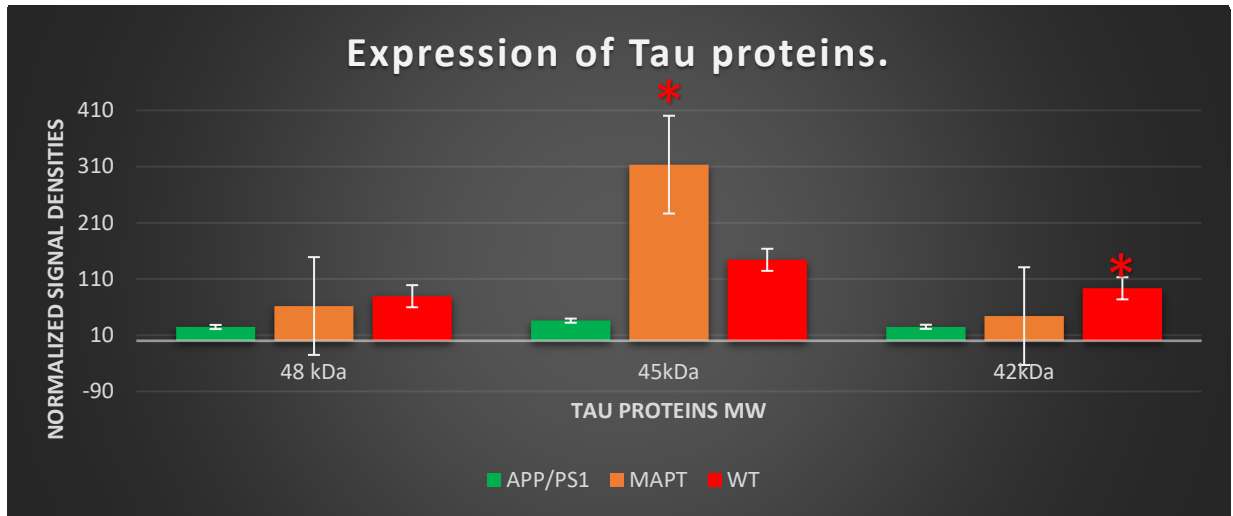


Figure 4.4: Strain Differences in Tau Isoforms. Isoform 45 was expressed significantly in MAPT mice, while expression in APP/PS1 was not significant to any isoforms and WT showed a predilection to isoform 42 expressions over other strain types.

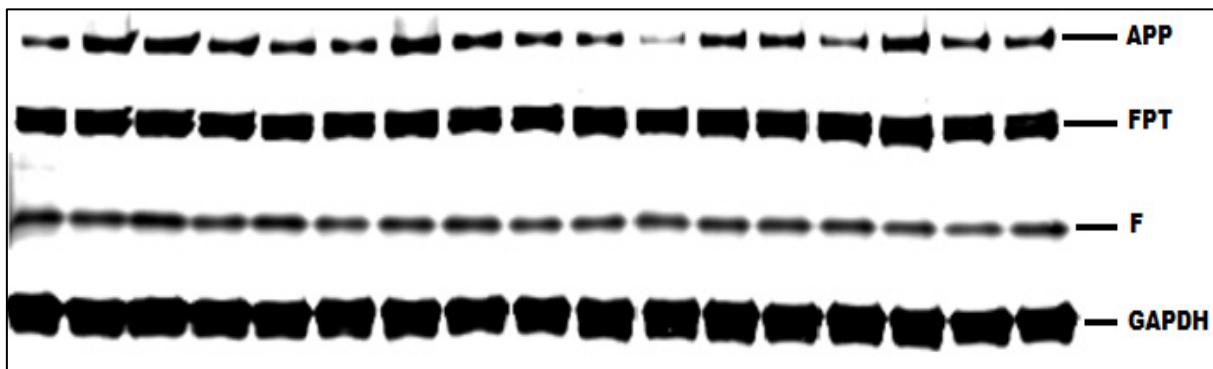


Figure 4.5: APP/PS1 Response to Oxidative Stress. Ultra-centrifuged brain homogenate extract were separated by SDS PAGE and probed with respective antibodies as described in Methods. Expression of ferritin, ferroportin and APP in APP/PS1 mice compared and normalized to GAPDH.

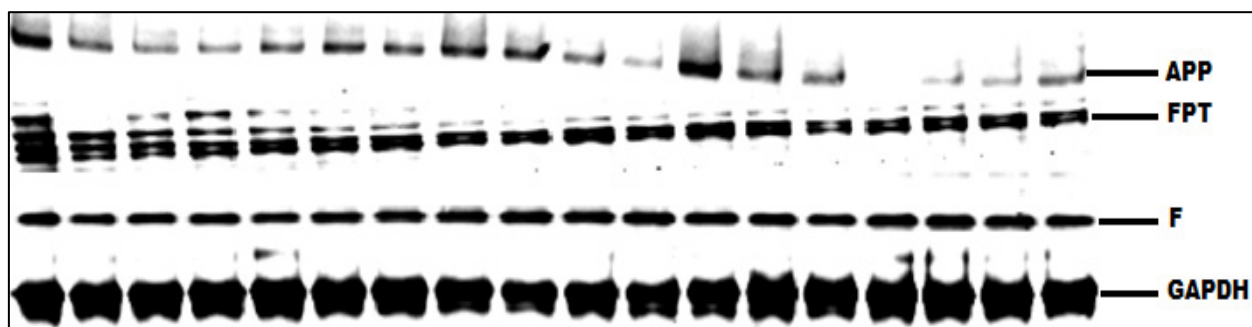


Figure 4.6: MAPT Response to Oxidative Stress. Ultra-centrifuged brain homogenate extract were separated by SDS PAGE and probed with respective antibodies as described in Methods. Expression of ferritin, ferroportin and APP in MAPT mice compared and normalized to GAPDH.

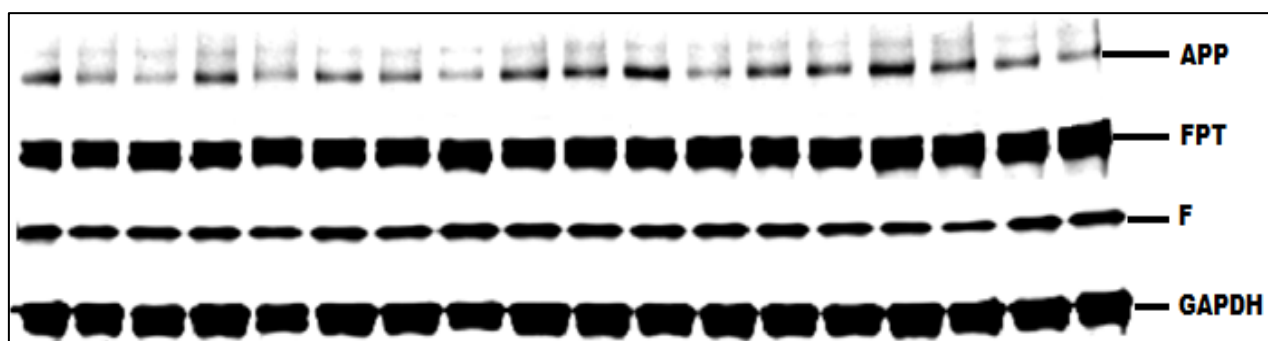


Figure 4.7: WT Response to Oxidative Stress. Ultra-centrifuged brain homogenate extract were separated by SDS PAGE and probed with respective antibodies as described in Methods. Expression of ferritin, ferroportin and APP in WT mice compared and normalized to GAPDH.

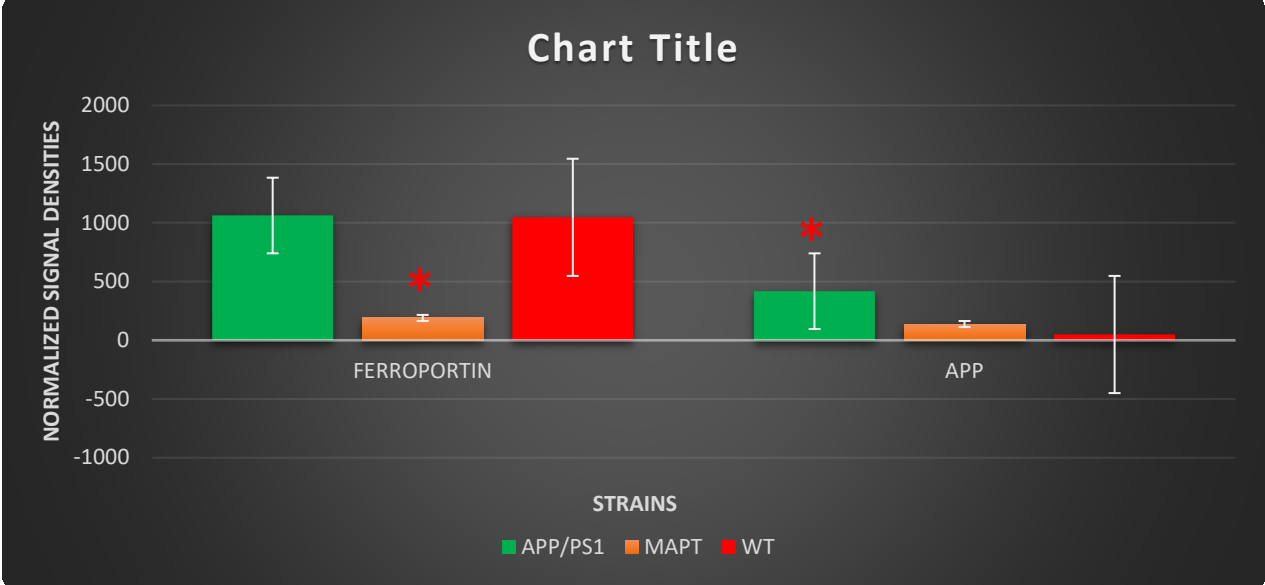


Figure 4.8: Strain’s Response to Oxidative Stress. Ferroportin was significantly under expressed in MAPT strain while APP/PS1 and WT showed marked expression following oxidative stress. APP is significantly over expressed in APP/PS1.

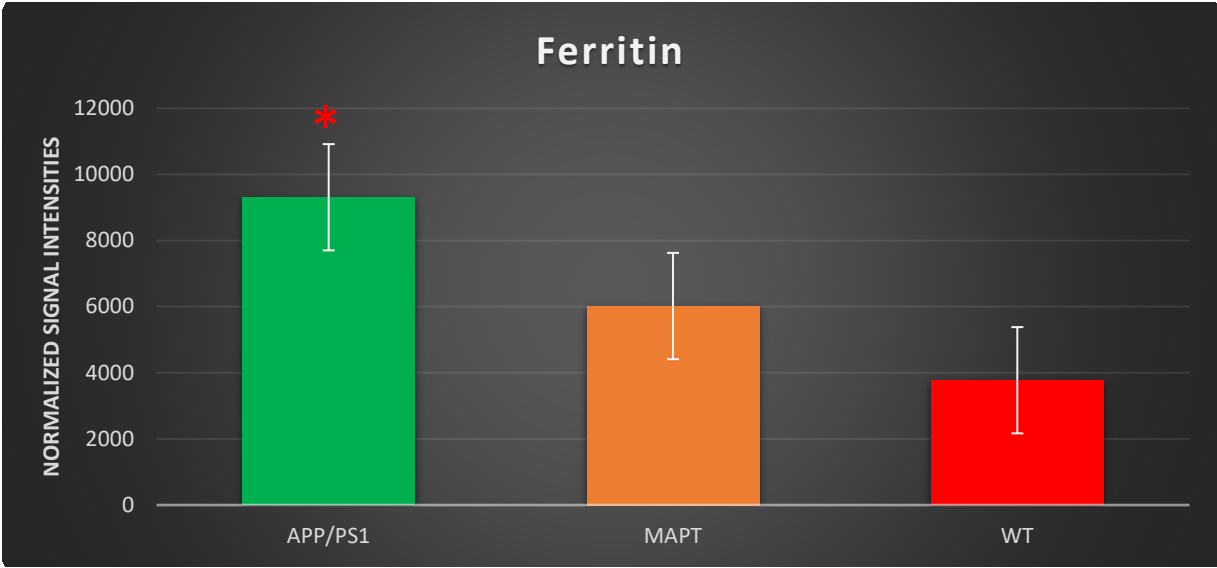


Figure 4.9: Ferritin Expression by Strain Type. APP/PS1 strain showed significant increase in ferritin expression over MAPT and WT.

Discussion

The complexities of tau isoform's role in various pathologies are variable, so, exclusive classification of tauopathies is challenging. Though, there are some studies attempting to attribute a particular isoform or group of isoforms responsible for pathogenesis, we are reporting various tau proteins with different molecular weight expressed with significance between cohorts. Expression of other proteins like ferritin (F), ferroportin (Fpt) and amyloid precursor protein (APP) are also discussed along with their possible interaction with various tau isoforms. While MAPT mice were able to produce all six isoforms, tau45 was expressed significantly higher ($P=0.022$) in MAPT than APP/PS1 and WT. However, the expression of tau48 and tau42 were not significant, in-fact, tau42 was significantly higher in WT than other strains including MAPT. This explains the complicated variation in isoforms expressions and pathology. As a response to oxidative stress treatment, APP/PS1 mice, along with their transgenic inclination, started producing amyloid beta to counteract the pathology. Significant increase in ferritin expression alone was not sufficient to keep iron sequestered, which is why APP production increased to make more amyloid beta. Subsequently, ferroportin expression also rose to shuttle iron complexed amyloid beta out of cell. The pathogenesis seems to be addressed by amyloid beta only, which is why expression of any isoform of tau was significantly lower or insignificant to other strain types. This activity describes our hypothesis of iron mediated oxidative stress and up regulation of these proteins to limit damages. Similarly, MAPT mice were programmed to produce all six isoform of human tau proteins. However, in response to oxidative stress, these particular strain types produced significant amounts of tau45. Since they were already programmed to produce hyper-phosphorylated tau, which could sequester iron and limit ROS mediated damage; APP expression was significantly lower than in APP/PS1 and WT mice.

Hyper-phosphorylated tau sequesters iron and forms intracellular neurofibrillary tangles, thereby limiting the roles of APP and ferroportin, which were found expressed significantly lower than APP/PS1 types. However, the expression of ferritin was lower than that seen with APP/PS1. Although, we do not fully understand the affinity of iron between hyper-phosphorylated tau and ferritin, the pathogenesis and expression of these proteins fits our iron hypothesis model. When we compared the pathogenesis with WT, which were not programmed to produce any particular proteins in dominance, we found expression of tau42 in significantly higher levels than other strains, including MAPT. However, the expression of APP was significantly lower and ferroportin was equally expressed as APP/PS1. Since the expression of amyloid beta could not be reported, it would be interesting to compare the pathological burden among strains, especially to address the temporal dynamics of our hypothesis. Higher expression of ferroportin in WT is likely related to upregulation of APP and ferritin, as they share common regulating pathways involving iron response element and iron response protein. Our findings have a strong base to support the hypothesis we put forward and we will be updating our findings from western blot for amyloid beta and histological confirmation.

Acknowledgements

The authors wish to thank the following funding sources: NIH/NIA 1 R21 AG037843; Brigham Young University, College of Life Sciences, Mentoring Environment Grant; Brigham Young University, School of Family Life, Gerontology Program; Brigham Young University, Magnetic Resonance Imaging Research Facility Seed Grant; Dr. Sarah M. McGinty Neuroscience Graduate Student Research Fellowship; Neurodar, LLC; Limitless Worldwide, LLC.

References

- Adam-Vizi, V. (2005). "Production of reactive oxygen species in brain mitochondria: contribution by electron transport chain and non-electron transport chain sources." *Antioxid Redox Signal* 7(9-10): 1140-1149.
- Aisen, P., C. Enns and M. Wessling-Resnick (2001). "Chemistry and biology of eukaryotic iron metabolism." *Int J Biochem Cell Biol* 33(10): 940-959.
- Behl, C., J. B. Davis, R. Lesley and D. Schubert (1994). "Hydrogen peroxide mediates amyloid beta protein toxicity." *Cell* 77(6): 817-827.
- Bush, A. I., C. S. Atwood, L. E. Goldstein, X. Huang and J. Rogers (2000). "Could Abeta and AbetaPP be Antioxidants?" *J Alzheimers Dis* 2(2): 83-84.
- Connor, J. R., S. L. Menzies, S. M. St Martin and E. J. Mufson (1992). "A histochemical study of iron, transferrin, and ferritin in Alzheimer's diseased brains." *J Neurosci Res* 31(1): 75-83.
- Finch, C. A. and H. Huebers (1982). "Perspectives in iron metabolism." *N Engl J Med* 306(25): 1520-1528.
- Good, P. F., D. P. Perl, L. M. Bierer and J. Schmeidler (1992). "Selective accumulation of aluminum and iron in the neurofibrillary tangles of Alzheimer's disease: a laser microprobe (LAMMA) study." *Ann Neurol* 31(3): 286-292.
- Haass, C., M. G. Schlossmacher, A. Y. Hung, C. Vigo-Pelfrey, A. Mellon, B. L. Ostaszewski, I. Lieberburg, E. H. Koo, D. Schenk, D. B. Teplow and et al. (1992). "Amyloid beta-peptide is produced by cultured cells during normal metabolism." *Nature* 359(6393): 322-325.
- Hensley, K., J. M. Carney, M. P. Mattson, M. Aksenova, M. Harris, J. F. Wu, R. A. Floyd and D. A. Butterfield (1994). "A model for beta-amyloid aggregation and neurotoxicity based on free radical generation by the peptide: relevance to Alzheimer disease." *Proc Natl Acad Sci U S A* 91(8): 3270-3274.
- Mattson, M. P. (1995). "Free radicals and disruption of neuronal ion homeostasis in AD: a role for amyloid beta-peptide?" *Neurobiol Aging* 16(4): 679-682; discussion 683.
- Menendez-Gonzalez, M., P. Perez-Pinera, M. Martinez-Rivera, M. T. Calatayud and B. Blazquez Menes (2005). "APP processing and the APP-KPI domain involvement in the amyloid cascade." *Neurodegener Dis* 2(6): 277-283.
- Nunomura, A., G. Perry, M. A. Pappolla, R. P. Friedland, K. Hirai, S. Chiba and M. A. Smith (2000). "Neuronal oxidative stress precedes amyloid-beta deposition in Down syndrome." *J Neuropathol Exp Neurol* 59(11): 1011-1017.

- Pratico, D., K. Uryu, S. Leight, J. Q. Trojanoswki and V. M. Lee (2001). "Increased lipid peroxidation precedes amyloid plaque formation in an animal model of Alzheimer amyloidosis." *J Neurosci* 21(12): 4183-4187.
- Reddy, P. H. and M. F. Beal (2005). "Are mitochondria critical in the pathogenesis of Alzheimer's disease?" *Brain Res Brain Res Rev* 49(3): 618-632.
- Reddy, P. H. and S. McWeeney (2006). "Mapping cellular transcriptosomes in autopsied Alzheimer's disease subjects and relevant animal models." *Neurobiol Aging* 27(8): 1060-1077.
- Selkoe, D. J. (2001). "Alzheimer's disease: genes, proteins, and therapy." *Physiol Rev* 81(2): 741-766.
- Selkoe, D. J., M. B. Podlisny, C. L. Joachim, E. A. Vickers, G. Lee, L. C. Fritz and T. Oltersdorf (1988). "Beta-amyloid precursor protein of Alzheimer disease occurs as 110- to 135-kilodalton membrane-associated proteins in neural and nonneural tissues." *Proc Natl Acad Sci U S A* 85(19): 7341-7345.
- Shoji, M., T. E. Golde, J. Ghiso, T. T. Cheung, S. Estus, L. M. Shaffer, X. D. Cai, D. M. McKay, R. Tintner, B. Frangione and et al. (1992). "Production of the Alzheimer amyloid beta protein by normal proteolytic processing." *Science* 258(5079): 126-129.
- Tanzi, R. E. and L. Bertram (2005). "Twenty years of the Alzheimer's disease amyloid hypothesis: a genetic perspective." *Cell* 120(4): 545-555.
- Theil, E. C. (2004). "Iron, ferritin, and nutrition." *Annu Rev Nutr* 24: 327-343.
- Wong, B. X., A. Tsatsanis, L. Q. Lim, P. A. Adlard, A. I. Bush and J. A. Duce (2014). "beta-Amyloid precursor protein does not possess ferroxidase activity but does stabilize the cell surface ferrous iron exporter ferroportin." *PLoS One* 9(12): e114174.
- Yan, S. D., S. F. Yan, X. Chen, J. Fu, M. Chen, P. Kuppusamy, M. A. Smith, G. Perry, G. C. Godman, P. Nawroth and et al. (1995). "Non-enzymatically glycosylated tau in Alzheimer's disease induces neuronal oxidant stress resulting in cytokine gene expression and release of amyloid beta-peptide." *Nat Med* 1(7): 693-699.

CHAPTER 5: General Conclusion and Relevance of Research

Our results strongly support the model for our iron hypothesis in initiation and progression of Alzheimer's disease. T2 weighted MR signal dropout in hippocampi seen by three months, strongly correlates with disease pathology and iron accumulation. This serves as a reference for developing better imaging sequences to improve signal-to-noise ratio in the future. In addition, this study highlights early pathogenesis, which facilitates future investigations to be conducted in the near future. Zinc concentration and its role at various oxidative conditions was interesting. Our study informs that the concentration of zinc, widely used for short-term (few weeks) studies may have reported benefitting outcomes, however, the same dosage for months (>three month) could be toxic to neurons. However, these finding demands further investigation as zinc is known to have dual effect in promoting and reducing amyloid plaques. Lastly, western blot results also supported our model for iron hypothesis. It was an interesting observation to see how different strain types, with predisposed conditions produced certain type of tau proteins, act differently but still in accordance to our iron hypothesis model.

While we could not comment on amyloid beta status, our next step is to follow up with western blot experiment on these proteins, and conformational histopathological studies looking for correlations between iron and proteins related to this disease. With so much of information inclining towards our hypothesis, we believe these remaining experiments will consolidate our finding in proving our hypothesis true.

Appendix 1: T2 Signal Intensities Measurements from Bilateral Hippocampi and Eyes from All Strains of Mice at One, Month.

Strain	Oxidative Treatment	Rescue Treatment	Mouse ID	Gender	Age	ONE MONTH			
						Left HPC	Right HPC	Left Eye	Right eye
APP/PS1	H	H	1	F	9	26.054	29.722	133	135
APP/PS1	H	H	2	M	6	29.684	25.114	32	30
APP/PS1	H	M	3	F	9	22.139	21.541	99	98
APP/PS1	H	M	4	F	6	17.921	18.833	79	86
APP/PS1	H	C	5	F	9	22.472	22.923	71	75
APP/PS1	H	C	6	F	6	26.861	25.444	108	100
APP/PS1	H	Z	7	F	9	29.973	24.444	136	130
APP/PS1	H	Z	8	F	6	33.351	32.632	170	169
APP/PS1	N	Z	9	M	9	30.919	27.658	157	166
APP/PS1	N	Z	10	M	6	33.444	32.5	164	169
APP/PS1	N	-	11	M	3	25.684	24.028	116	117
APP/PS1	N	N	12	M	9	27.865	26.077	162	159
APP/PS1	N	N	13	M	6	20.917	18.222	127	119
APP/PS1	N	C	14	F	9	28.795	26.667	118	126
APP/PS1	N	C	15	F	6	24.417	23.514	140	143
APP/PS1	H	-	16	M	3	27.325	28.135	129	137
APP/PS1	N	M	17	F	6	23.947	22.139	89	80
APP/PS1	N	M	18	M	9	24.216	20.649	138	140
MAPT	N	N	40	M	9	29.314	28.051	153	136
MAPT	N	N	41	M	6	29.947	30.595	194	188
MAPT	H	H	46	F	9	19.622	23.868	78	77
MAPT	H	H	47	F	6	28.5	25.053	47	58
MAPT	H	M	48	M	9	29.027	30.028	120	122
MAPT	H	M	49	M	6	27.865	30.086	141	140
MAPT	H	C	53	F	9	24.324	20.2	102	110
MAPT	H	C	54	F	6	28.875	30.865	159	147
MAPT	H	Z	55	F	9	25.447	22.784	122	134
MAPT	H	Z	56	F	6	29.921	33.056	132	139
MAPT	H	-	57	F	3	25.806	28.622	147	149
MAPT	N	-	58	M	3	30.75	25.972	144	139
MAPT	N	M	59	F	9	26.056	25.184	156	151
MAPT	N	M	60	F	6	18.784	17.919	113	105

Appendix 1 continued.

Strain	Oxidative Treatment	Rescue Treatment	Mouse ID	Gender	Age	ONE MONTH			
						Left HPC	Right HPC	Left Eye	Right eye
MAPT	N	C	61	M	9	32.114	31.944	165	167
MAPT	N	C	62	M	6	30.171	30.528	166	168
MAPT	N	Z	64	F	9	22.579	21.5	131	119
MAPT	N	Z	65	F	6	20.4	20.324	130	124
WT	N	N	16	M	9	26.722	27.194	131	129
WT	N	N	17	M	6	29.974	28.108	153	152
WT	H	M	20	M	6	32.514	32.079	148	149
WT	H	M	21	M	9	26	24.158	141	138
WT	H	C	22	M	6	21.757	19.757	128	109
WT	H	C	23	M	9	19.029	17.462	133	125
WT	H	Z	29	M	9	26.946	28.526	123	142
WT	H	Z	30	M	6	22.568	24.579	128	115
WT	H	H	31	M	9	24.526	27.579	136	152
WT	H	H	32	M	6	35.703	32.081	99	104
WT	N	C	33	F	9	27.972	27.194	141	163
WT	N	M	34	M	9	25.865	25.73	114	125
WT	N	M	35	M	6	14.361	13.343	96	104
WT	N	-	36	M	3	30.763	29.676	110	124
WT	N	Z	46	F	9	19.868	20.054	124	116
WT	N	Z	47	F	6	25.27	23.833	101	96
WT	N	C	48	F	6	26.861	27.343	117	116
WT	H	-	49	M	3	22.056	20.167	135	138

Appendix 2: T2 Signal Intensities Measurements from Bilateral Hippocampi and Eyes from All Strains of Mice at Three, Month.

						THREE MONTHS			
Strain	Oxidative Treatment	Rescue Treatment	Mouse ID	Gender	Age	Left HPC	Right HPC	Left Eye	Right eye
APP/PS1	H	H	1	F	9	28.806	26.079	154	152
APP/PS1	H	H	2	M	6	27.676	26.722	142	142
APP/PS1	H	M	3	F	9	32.556	31.811	162	190
APP/PS1	H	M	4	F	6	26.886	24.649	166	163
APP/PS1	H	C	5	F	9	31.694	29.667	158	150
APP/PS1	H	C	6	F	6	26.575	26.5	145	147
APP/PS1	H	Z	7	F	9	11.079	10.868	90	79
APP/PS1	H	Z	8	F	6	24	27.737	123	135
APP/PS1	N	Z	9	M	9	19.784	18.65	122	151
APP/PS1	N	Z	10	M	6	27.361	25.184	147	143
APP/PS1	N	-	11	M	3	25.162	23.514	189	159
APP/PS1	N	N	12	M	9	23.4	22.806	150	154
APP/PS1	N	N	13	M	6	24.128	21.784	162	145
APP/PS1	N	C	14	F	9	22.167	23.143	111	120
APP/PS1	N	C	15	F	6	23.389	19.921	148	148
APP/PS1	H	-	16	M	3	18.639	19.081	135	125
APP/PS1	N	M	17	F	6	28.917	27.432	142	137
APP/PS1	N	M	18	M	9	20.421	20.5	149	149
MAPT	N	N	40	M	9	28.868	27.368	167	153
MAPT	N	N	41	M	6	24.316	22.526	138	149
MAPT	H	H	46	F	9	28.694	24.028	159	157
MAPT	H	H	47	F	6	23.914	20.306	156	142
MAPT	H	M	48	M	9	33.105	29.75	205	205
MAPT	H	M	49	M	6	27.083	27.385	170	177
MAPT	H	C	53	F	9	28.5	25.343	150	158
MAPT	H	C	54	F	6	28.622	26.763	159	163
MAPT	H	Z	55	F	9	30.27	26.135	174	162
MAPT	H	Z	56	F	6	29.054	27.444	176	161
MAPT	H	-	57	F	3	30.684	28.737	178	169
MAPT	N	-	58	M	3	23.421	22.784	123	126
MAPT	N	M	59	F	9	25.5	24.514	154	167
MAPT	N	M	60	F	6	27.816	28.026	140	148
MAPT	N	C	61	M	9	19.081	18.189	126	119

Appendix 2 continued.

Strain	Oxidative Treatment	Rescue Treatment	Mouse ID	Gender	Age	THREE MONTHS			
						Left HPC	Right HPC	Left Eye	Right eye
MAPT	N	C	62	M	6	19.103	18.73	147	148
MAPT	N	Z	64	F	9	26.342	23.868	138	142
MAPT	N	Z	65	F	6	27.632	25.421	160	149
WT	N	N	16	M	9	26.105	26.605	166	166
WT	N	N	17	M	6	28.081	29.421	182	189
WT	H	M	20	M	6	35.703	31.459	178	202
WT	H	M	21	M	9	35.308	30.833	180	195
WT	H	C	22	M	6	31.105	29.658	161	185
WT	H	C	23	M	9	30.289	27.405	167	175
WT	H	Z	29	M	9	26.658	24.947	162	168
WT	H	Z	30	M	6	22.795	24.722	156	146
WT	H	H	31	M	9	18.806	19.316	144	135
WT	H	H	32	M	6	32.632	35.135	188	201
WT	N	C	33	F	9	22.472	21.556	139	132
WT	N	M	34	M	9	28.054	25.395	168	167
WT	N	M	35	M	6	27.889	25.5	167	166
WT	N	-	36	M	3	18.154	17.737	118	124
WT	N	Z	46	F	9	28.944	29.622	163	151
WT	N	Z	47	F	6	17.806	18.868	143	134
WT	N	C	48	F	6	25.395	27.289	170	168
WT	H	-	49	M	3	27.529	27.447	166	157

Appendix 3: T2 Signal Intensities Measurements from Bilateral Hippocampi and Eyes from All Strains of Mice at Six, Month.

Strain	Oxidative Treatment	Rescue Treatment	Mouse ID	Gender	Age	SIX MONTHS			
						Left HPC	Right HPC	Left Eye	Right eye
APP/PS1	H	H	1	F	9	25.639	25.75	140	144
APP/PS1	H	H	2	M	6	24.028	23.971	138	153
APP/PS1	H	M	3	F	9	28.75	30.474	137	151
APP/PS1	H	M	4	F	6	23.486	20.975	147	141
APP/PS1	H	C	5	F	9	20.189	19.077	146	150
APP/PS1	H	C	6	F	6	25.211	26.447	190	174
APP/PS1	H	Z	7	F	9	25	24.743	150	150
APP/PS1	H	Z	8	F	6	26.917	27.351	172	174
APP/PS1	N	Z	9	M	9	20.257	19.972	123	136
APP/PS1	N	Z	10	M	6	17.811	16.25	90	101
APP/PS1	N	-	11	M	3				
APP/PS1	N	N	12	M	9	13.108	10.897	68	61
APP/PS1	N	N	13	M	6	22.167	21.472	139	127
APP/PS1	N	C	14	F	9	21.568	20.686	149	151
APP/PS1	N	C	15	F	6	16.278	13.405	104	106
APP/PS1	H	-	16	M	3				
APP/PS1	N	M	17	F	6	29.892	25.865	162	174
APP/PS1	N	M	18	M	9	23.917	18.632	168	171
MAPT	N	N	40	M	9	31.639	29.639	162	166
MAPT	N	N	41	M	6	18.371	18.676	131	135
MAPT	H	H	46	F	9	21.861	18.395	150	134
MAPT	H	H	47	F	6	23.568	23.944	124	143
MAPT	H	M	48	M	9	18.5	16.694	130	133
MAPT	H	M	49	M	6	21.444	19.974	167	141
MAPT	H	C	53	F	9	25.028	23.139	142	138
MAPT	H	C	54	F	6	23	17.526	162	158
MAPT	H	Z	55	F	9	14.833	15.846	113	109
MAPT	H	Z	56	F	6	17.703	15.395	130	119
MAPT	H	-	57	F	3				
MAPT	N	-	58	M	3				
MAPT	N	M	59	F	9	16.667	17.108	124	132
MAPT	N	M	60	F	6	21.056	20.108	136	134
MAPT	N	C	61	M	9	17.861	18.5	128	132

Appendix 3 continued.

Strain	Oxidative Treatment	Rescue Treatment	Mouse ID	Gender	Age	SIX MONTHS			
						Left HPC	Right HPC	Left Eye	Right eye
MAPT	N	C	62	M	6	20.925	21.333	161	145
MAPT	N	Z	64	F	9	25.361	25.889	172	166
MAPT	N	Z	65	F	6	26.541	25.649	146	148
WT	N	N	16	M	9	23.861	22.528	175	174
WT	N	N	17	M	6	28.947	26.111	213	195
WT	H	M	20	M	6	26.842	26.579	176	164
WT	H	M	21	M	9	26.056	22.514	145	153
WT	H	C	22	M	6	15.875	15.333	111	109
WT	H	C	23	M	9	15.556	15.514	116	115
WT	H	Z	29	M	9	30.811	29.029	175	176
WT	H	Z	30	M	6	25.861	25.5	178	166
WT	H	H	31	M	9	22.943	26.278	148	161
WT	H	H	32	M	6	24.429	21.778	147	148
WT	N	C	33	F	9	19.611	18	78	68
WT	N	M	34	M	9	22.308	20.684	142	144
WT	N	M	35	M	6	13.351	13.395	76	74
WT	N	-	36	M	3				
WT	N	Z	46	F	9	25.694	26.351	161	161
WT	N	Z	47	F	6	27.306	29.162	171	179
WT	N	C	48	F	6	22.361	21.297	162	172
WT	H	-	49	M	3				

Appendix 4: T2 Signal Intensities Measurements from Bilateral Hippocampi and Eyes from All Strains of Mice at Nine, Month.

Strain	Oxidative Treatment	Rescue Treatment	Mouse ID	Gender	Age	NINE MONTHS			
						Left HPC	Right HPC	Left Eye	Right eye
APP/PS1	H	H	1	F	9	31.111	30.056	192	175
APP/PS1	H	H	2	M	6				
APP/PS1	H	M	3	F	9	27.351	30	157	167
APP/PS1	H	M	4	F	6				
APP/PS1	H	C	5	F	9	25.351	24.026	169	162
APP/PS1	H	C	6	F	6				
APP/PS1	H	Z	7	F	9	21.686	22	154	152
APP/PS1	H	Z	8	F	6				
APP/PS1	N	Z	9	M	9	18.75	17.105	125	118
APP/PS1	N	Z	10	M	6				
APP/PS1	N	-	11	M	3				
APP/PS1	N	N	12	M	9	20.806	22.972	156	156
APP/PS1	N	N	13	M	6				
APP/PS1	N	C	14	F	9	24.917	20.744	141	147
APP/PS1	N	C	15	F	6				
APP/PS1	H	-	16	M	3				
APP/PS1	N	M	17	F	6				
APP/PS1	N	M	18	M	9	24.757	24.054	126	141
MAPT	N	N	40	M	9	21.421	15.778	141	158
MAPT	N	N	41	M	6				
MAPT	H	H	46	F	9	19.829	18.189	146	179
MAPT	H	H	47	F	6				
MAPT	H	M	48	M	9	21.189	19.27	150	138
MAPT	H	M	49	M	6				
MAPT	H	C	53	F	9	23.789	24.865	174	172
MAPT	H	C	54	F	6				
MAPT	H	Z	55	F	9	20.486	16.711	117	123
MAPT	H	Z	56	F	6				
MAPT	H	-	57	F	3				
MAPT	N	-	58	M	3				
MAPT	N	M	59	F	9	20.211	17.543	128	136
MAPT	N	M	60	F	6				
MAPT	N	C	61	M	9	24.946	24.514	194	170

Appendix 4 continued.

Strain	Oxidative Treatment	Rescue Treatment	Mouse ID	Gender	Age	NINE MONTHS			
						Left HPC	Right HPC	Left Eye	Right eye
MAPT	N	C	62	M	6				
MAPT	N	Z	64	F	9	26.306	24.658	160	148
MAPT	N	Z	65	F	6				
WT	N	N	16	M	9	14.526	14.306	51	47
WT	N	N	17	M	6				
WT	H	M	20	M	6				
WT	H	M	21	M	9	19.615	18.556	130	143
WT	H	C	22	M	6				
WT	H	C	23	M	9	21.5	22.27	148	155
WT	H	Z	29	M	9	29	26.8	155	164
WT	H	Z	30	M	6				
WT	H	H	31	M	9	22.763	21.154	148	146
WT	H	H	32	M	6				
WT	N	C	33	F	9	27.297	25.861	174	168
WT	N	M	34	M	9	17.487	15.861	110	114
WT	N	M	35	M	6				
WT	N	-	36	M	3				
WT	N	Z	46	F	9	28.128	27.184	180	185
WT	N	Z	47	F	6				
WT	N	C	48	F	6				
WT	H	-	49	M	3				

Appendix 5: T1 and T2 Measurements on Ultra-Centrifuged Mice Brain Homogenates for APP/PS1 Mice at Three, Six and Nine Months.

Strain	Oxidative Treatment	Rescue Treatment	Mouse ID	Gender	Age	T1	T2
APP/PS1	H	H	1	F	9	6.46	3.15
APP/PS1	H	M	3	F	9	7.28	3.12
APP/PS1	H	M	4	F	6	6.57	2.97
APP/PS1	H	C	5	F	9	6.67	3.15
APP/PS1	H	C	6	F	6	6.53	3.01
APP/PS1	H	Z	7	F	9	6.51	2.83
APP/PS1	H	Z	8	F	6	6.67	2.99
APP/PS1	N	Z	9	M	9	4.29	1.43
APP/PS1	N	Z	10	M	6	5.92	2.83
APP/PS1	N	-	11	M	3	6.28	2.99
APP/PS1	N	N	12	M	9	6.37	2.94
APP/PS1	N	N	13	M	6	5.95	2.83
APP/PS1	N	C	14	F	9	6.71	2.98
APP/PS1	N	C	15	F	6	7.11	3.02
APP/PS1	H	-	16	M	3	7.78	2.9
APP/PS1	N	M	17	F	6	7.39	3.44
APP/PS1	N	M	18	M	9	6.29	3.02

Appendix 6: T1 and T2 Measurements on Ultra-Centrifuged Mice Brain Homogenates for MAPT Mice at Three, Six and Nine Months.

Strain	Oxidative Treatment	Rescue Treatment	Mouse ID	Gender	Age	T1	T2
MAPT	N	N	40	M	9	6.6	2.78
MAPT	N	N	41	M	6	6.16	2.82
MAPT	H	H	46	F	9	6.57	2.74
MAPT	H	H	47	F	6	6.4	2.91
MAPT	H	M	48	M	9	6.63	3.08
MAPT	H	M	49	M	6	6.35	2.94
MAPT	H	C	53	F	9	6.26	2.91
MAPT	H	C	54	F	6	5.95	2.63
MAPT	H	Z	55	F	9	6.07	2.99
MAPT	H	Z	56	F	6	6.55	2.88
MAPT	H	-	57	F	3	6.6	2.92
MAPT	N	-	58	M	3	6.35	2.82
MAPT	N	M	59	F	9	6.71	2.83
MAPT	N	M	60	F	6	6.15	2.79
MAPT	N	C	61	M	9	6.37	2.89
MAPT	N	C	62	M	6	7.65	2.69
MAPT	N	Z	64	F	9	6.95	2.86
MAPT	N	Z	65	F	6	7.1	2.81

Appendix 7: T1 and T2 Measurements on Ultra-Centrifuged Mice Brain Homogenates for WT Mice at Three, Six and Nine Months.

Strain	Oxidative Treatment	Rescue Treatment	Mouse ID	Gender	Age	T1	T2
WT	N	N	16	M	9	6.79	2.99
WT	N	N	17	M	6	4.68	1.81
WT	H	M	20	M	6	6.48	2.74
WT	H	M	21	M	9	6.52	2.93
WT	H	C	22	M	6	6.18	2.77
WT	H	C	23	M	9	7.66	3.19
WT	H	Z	29	M	9	6.35	2.89
WT	H	Z	30	M	6	6.48	2.93
WT	H	H	31	M	9	6.4	2.84
WT	H	H	32	M	6	6.56	2.85
WT	N	C	33	F	9	6.49	2.92
WT	N	M	34	M	9	6.51	2.89
WT	N	M	35	M	6	6.8	2.94
WT	N	-	36	M	3	6.47	2.93
WT	N	Z	46	F	9	6.64	2.93
WT	N	Z	47	F	6	4.53	1.49
WT	N	C	48	F	6	6.65	3.04
WT	H	-	49	M	3	6.61	3.13

Appendix 8: Ultra-Centrifuged Mice Brain Homogenates Were Run On SDS PAGE Gel And Were Probed And Density Measured For Following Proteins: APP, Ferritin, Ferroportin And GAPDH.

	Oxidative Treatment	Rescue Treatment	Mouse ID	Gender	Age	GAPDH	Ferritin	Fpn	APP
APP/PS1	H	H	1	F	9	24000	10800	1020	204
APP/PS1	H	M	3	F	9	24400	10200	689	461
APP/PS1	H	M	4	F	6	26000	14200	959	452
APP/PS1	H	C	5	F	9	21700	9910	803	341
APP/PS1	H	C	6	F	6	20200	11500	754	256
APP/PS1	H	Z	7	F	9	20500	8390	722	257
APP/PS1	H	Z	8	F	6	19100	10200	879	483
APP/PS1	N	Z	9	M	9	20400	10900	633	361
APP/PS1	N	Z	10	M	6	20200	8130	665	267
APP/PS1	N	-	11	M	3	16000	8690	918	243
APP/PS1	N	N	12	M	9	18700	8710	617	146
APP/PS1	N	N	13	M	6	21700	8990	855	280
APP/PS1	N	C	14	F	9	24100	8970	722	290
APP/PS1	N	C	15	F	6	30800	9470	942	220
APP/PS1	H	-	16	M	3	24800	8110	774	374
APP/PS1	N	M	17	F	6	30300	7090	572	266
APP/PS1	N	M	18	M	9	29900	10300	563	298
MAPT	N	N	40	M	9	1200	136	113	131
MAPT	N	N	41	M	6	1060	89.3	66.3	90.5
MAPT	H	H	46	F	9	1260	114	90.7	87.8
MAPT	H	H	47	F	6	1130	117	125	79.3
MAPT	H	M	48	M	9	1310	98.6	139	93
MAPT	H	M	49	M	6	989	125	127	112
MAPT	H	C	53	F	9	973	131	143	102
MAPT	H	C	54	F	6	906	156	132	122
MAPT	H	Z	55	F	9	928	178	130	150
MAPT	H	Z	56	F	6	1030	167	192	88.1
MAPT	H	-	57	F	3	797	185	134	54.2
MAPT	N	-	58	M	3	854	147	185	161
MAPT	N	M	59	F	9	820	140	166	104
MAPT	N	M	60	F	6	1090	114	122	83.8
MAPT	N	C	61	M	9	1110	163	123	29.1
MAPT	N	C	62	M	6	1060	185	127	75.9

Appendix 8 continued.

Strain	Oxidative Treatment	Rescue Treatment	Mouse ID	Gender	Age	GAPDH	Ferritin	Fpn	APP
MAPT	N	Z	64	F	9	1140	164	124	72.4
MAPT	N	Z	65	F	6	1470	147	141	96.6
WT	N	N	16	M	9	26800	4430	605	43.9
WT	N	N	17	M	6	23600	3640	474	24.9
WT	H	M	20	M	6	25000	4360	817	16.9
WT	H	M	21	M	9	32400	4530	650	42.6
WT	H	C	22	M	6	18000	3210	528	16.9
WT	H	C	23	M	9	30400	4970	766	39.8
WT	H	Z	29	M	9	26200	4510	764	35.1
WT	H	Z	30	M	6	18900	6350	663	24.2
WT	H	H	31	M	9	28600	5660	917	52.5
WT	H	H	32	M	6	21900	4970	868	48.5
WT	N	C	33	F	9	25300	4790	994	62
WT	N	M	34	M	9	24500	5030	994	29
WT	N	M	35	M	6	24600	4940	826	48.2
WT	N	-	36	M	3	27100	4330	826	45.2
WT	N	Z	46	F	9	29100	3910	1180	61.5
WT	N	Z	47	F	6	28000	2710	1090	49.9
WT	N	C	48	F	6	30000	5220	941	41.1
WT	H	-	49	M	3	30500	5410	1250	35.8

Appendix 9: Ultra- Centrifuged Mice Brain Homogenates Were Run On SDS PAGE Gel And Were Probed For Various Following Proteins. Density Measurement of GAPDH for Tau and Different Tau Proteins Measured at 42, 45 And 48 kDa.

Strain	Oxidative Treatment	Rescue Treatment	Mouse ID	Gender	Age	GAPDH TAU	TAU-48	TAU-45	TAU-42
APP/PS1	H	H	1	F	9	11300	19.6	53.4	21.4
APP/PS1	H	M	3	F	9	9170	20.9	28	19
APP/PS1	H	M	4	F	6	11400	15.5	42.1	21.7
APP/PS1	H	C	5	F	9	9920	14.1	29.4	24.5
APP/PS1	H	C	6	F	6	8590	5.61	23.3	17.7
APP/PS1	H	Z	7	F	9	9090	14.4	30	29.7
APP/PS1	H	Z	8	F	6	9770	15.3	25.5	14.4
APP/PS1	N	Z	9	M	9	8700	17.5	28.3	16.6
APP/PS1	N	Z	10	M	6	10800	29.4	27.4	13.5
APP/PS1	N	-	11	M	3	9640	20.6	21.6	21.1
APP/PS1	N	N	12	M	9	8080	7.54	33	22.1
APP/PS1	N	N	13	M	6	10800	27.7	21.9	25.4
APP/PS1	N	C	14	F	9	10100	10.8	42.8	27.5
APP/PS1	N	C	15	F	6	10100	56.2	42.3	17.5
APP/PS1	H	-	16	M	3	8080	31.3	20.6	25.1
APP/PS1	N	M	17	F	6	8970	17	29.9	27.5
APP/PS1	N	M	18	M	9	11000	36.2	21.1	9.73
MAPT	N	N	40	M	9	8530	99.7	413	73.4
MAPT	N	N	41	M	6	8520	6.93	72.7	17
MAPT	H	H	46	F	9	10500	38.9	215	8.62
MAPT	H	H	47	F	6	6490	46.9	403	55.9
MAPT	H	M	48	M	9	8850	39.9	288	61.3
MAPT	H	M	49	M	6	7970	72.8	357	14.8
MAPT	H	C	53	F	9	8180	51.7	357	43.8
MAPT	H	C	54	F	6	9270	47.6	240	40.1
MAPT	H	Z	55	F	9	8210	46.6	254	47.8
MAPT	H	Z	56	F	6	8400	34.1	171	19.8
MAPT	H	-	57	F	3	8760	17.5	21.1	-11.3
MAPT	N	-	58	M	3	9540	21	143	13.9
MAPT	N	M	59	F	9	9560	34.5	271	90.2
MAPT	N	M	60	F	6	9660	49	298	47.1
MAPT	N	C	61	M	9	8910	37.5	90.8	7.91

Appendix 9 continued.

Strain	Oxidative Treatment	Rescue Treatment	Mouse ID	Gender	Age	GAPDH TAU	TAU-48	TAU-45	TAU-42
MAPT	N	C	62	M	6	10300	24.9	145	18.4
MAPT	N	Z	64	F	9	12100	29.7	166	5.03
MAPT	N	Z	65	F	6	10800	128	152	10.9
WT	N	N	16	M	9	8310	47.8	80	56
WT	N	N	17	M	6	5170	35.8	85.8	53.1
WT	H	M	20	M	6	7080	45.8	107	59.8
WT	H	M	21	M	9	8140	46.7	95.6	65
WT	H	C	22	M	6	4390	61.9	123	72.1
WT	H	C	23	M	9	8810	57.1	117	76.4
WT	H	Z	29	M	9	8760	58.7	124	65.3
WT	H	Z	30	M	6	7090	92.6	137	110
WT	H	H	31	M	9	11600	62.5	108	67.4
WT	H	H	32	M	6	9140	52.1	127	53.3
WT	N	C	33	F	9	11800	58.5	115	68.2
WT	N	M	34	M	9	10100	46.1	76.2	65
WT	N	M	35	M	6	10500	61.3	85.7	66.2
WT	N	-	36	M	3	9640	43.1	73.3	53.5
WT	N	Z	46	F	9	9630	60.3	82.7	54
WT	N	Z	47	F	6	10900	81.2	103	74
WT	N	C	48	F	6	10700	54.7	82.2	62
WT	H	-	49	M	3	10400	63.4	104	73.3

CURRICULUM VITAE

RAJAN DEEP ADHIKARI

1407 University Village, Salt Lake City, UT 84108. 208-789-8550. rajandeep@hotmail.com

EDUCATION

Doctor of Philosophy in Neuroscience; Physiology and Developmental Biology. Brigham Young University 2017

(*Dissertation*: MRI T2 Signal Changes Indicate Tau Pathophysiology in a Murine Alzheimer's disease Model)

Bachelor of Medicine, Bachelor of Surgery (MBBS); Kathmandu University. Nepal 2005

TEACHING EXPERIENCE

Teaching Assistant: Advanced Physiology. Brigham Young University 2013-2014
Instructed physiology coursework, delivered several lectures on human anatomy and physiology, assisted in lab-work, graded and reviewed final exams.

Instructor: Gross Anatomy. The University of Utah School of Medicine 2014
Instructed human gross anatomy to medical students, helped with dissection techniques and clinical applications of such learning.

General Physician: Kathmandu, Nepal. 2006-2012
Instructed and guided junior medical officers, nursing staffs and medical/nursing students in various aspects of clinical knowledge and practice. Assisted in various bedside procedures.

PROFESSIONAL EXPERIENCE

General Physician: Kathmandu, Nepal.
Practiced general medicine in various hospitals in Nepal. Delivered medical and minor surgical treatments to patients. Acquired skills and knowledge pertaining to practice of medicine.

RESEARCH EXPERIENCE

Research Assistant: Dr. Jonathan J. Wisco's Laboratory for Translational Anatomy of Degenerative Diseases and Developmental Disorders. Physiology and Developmental Biology, Neuroscience Center. Brigham Young University: 2013.

- Developed a hypothesis relating oxidative stress of iron on neurons and their direct relation to the development of pathological plaques associated with AD.
- Magnetic resonance imaging on transgenic APP/PS1 and Tau mice and measuring the signal dropout in region of interest and comparing that with controlled wild types.
- NMR study on brain homogenates of experimental animals and analyzing the relaxation properties.
- Western Blot of brain homogenates: to study the quality and relative quantity of proteins expression.
- Immunohistochemistry on mice brain. (Experiment not concluded).

Research Assistant: Dr. Jeffery Edward's Lab. Physiology and Developmental Biology. Brigham Young University: 2012-2013.

- Electrophysiological study of synaptic plasticity in VTA and Hippocampus.

GRANTS AND AWARDS

Neuroscience Fellowship: College of life science, BYU	2012-Present
Graduate research fellowship: Physiology and Developmental Biology. BYU	2014-2015
Gerontology Grant	2014
Graduate student funding through Physiology and Developmental Biology. BYU	2013

PEER REVIEW PUBLICATIONS

Hippocampal T2 Signal Loss During Aging in Transgenic Murine Modeled for AD Reflects Pathological Lesions, Rajan D. Adhikari¹, R. Staudte¹, M. Atmojo¹, M. Mendoza², H. Wang², R. Watt³, N. Bangerter², J. Wisco^{1,4}. ¹Department of Physiology and Developmental Biology, ²Department of Electrical Engineering, ³ Department of Chemistry and Biochemistry, Brigham Young University, Provo, UT. ⁴Department of Neurobiology and Anatomy, University of Utah Medical School, Salt Lake City, UT. (In Progress)

Strain Specific Regulation of Proteins: An Iron Hypothesis for Alzheimer's disease, Rajan D. Adhikari¹, R. Watt³, N. Bangerter², S. Burt³, J. Wisco^{1,4}. ¹Department of Physiology and Developmental Biology, ²Department of Electrical Engineering, ³ Department of Chemistry and Biochemistry, Brigham Young University, Provo, UT. ⁴Department of Neurobiology and Anatomy, University of Utah Medical School, Salt Lake City, UT. (In Progress)

Dual Role of Zinc: NMR Relaxometry Measurements on Pathological and Normal Murine Brain, Rajan D. Adhikari¹, R. Lee¹, K. Noorda¹, B. Ramfjord¹, S. Burt², R. Watt², J. Wisco, ¹Department of Physiology and Developmental Biology, ²Department of Electrical Engineering, ³ Department of Chemistry and Biochemistry, Brigham Young University, Provo, UT. ⁴Department of Neurobiology and Anatomy, University of Utah Medical School, Salt Lake City, UT. (In Progress)

CONFERENCE PRESENTATIONS

Rajan D. Adhikari, Cata Matias, Amin Nazaran, Kevin Perkins, Scott R. Burt, Ph.D., Neal Bangerter, Ph.D., Richard K. Watt, Ph.D., Jonathan J. Wisco, Ph.D. (2014). Can iron be used as a diagnostic biomarker for Alzheimer's disease? Poster presented at the annual BYU graduate expo, Provo, UT.

Rajan D. Adhikari, Scott R. Burt, Neal Bangerter, Richard K. Watt, H V Vinters, Jonathan J. Wisco. (2014). Relaxation properties of iron bound AD-associated proteins. Poster presented at Society for Neuroscience, Neuroscience 2014, Washington D.C.

Rajan D. Adhikari, Scott R. Burt, Neal Bangerter, Richard K. Watt, H V Vinters, Jonathan J. Wisco. (2015). Relaxation properties of iron bound AD-associated proteins. Poster presented at Alzheimer's Association, Washington D.C.

CREDENTIALS AND LICENSES

Graduate Record Examination (GRE)	2011
Test of English as Foreign Language (TOEFL)	2011
United States Medical Licensing Examination (USMLE): Steps I, II CK, II CS and III	2008
Education Commission for Foreign Medical Graduates (ECFMG)	2008
Nepal Medical Council	2005

PROFESSIONAL MEMBERSHIP

Society for Neuroscience	2014-present
Alzheimer's Association	2015-present